

# Rubber recycling Calender

Thesis



-280°C

-240°C

-200°C

-160°C

-120°C

-80°C

-40°C

Bachelor thesis

**Version 2.0**

Author: Peter-Bas Schelling

Student number: s1032900

E-mail: [pbschelling@gmail.com](mailto:pbschelling@gmail.com)

Education: Mechanical engineering

Organisation: Hogeschool Windesheim

Company supervisor: Hans van Hoek

School Supervisor: Niels Boks

Graduation period: February – August 2015

ISBN: 978-90-830591-6-7



## **RUBBER RECYCLING CALENDER SUMMARY**

---

An estimated 17 million tonnes of tires are discarded annually. Re-use is achieved by retreading (9%), recycling (39%), energy recovery (37%) and landfill (5%). A preferred, but complex way of recycling is to make new tires from discarded tire rubber.

Vulcanised car tire rubber has to be devulcanized before it can be re-used into car tire compounds. The department of Elastomer Technology and Engineering (ETE) of the University of Twente (UTwente) has developed a thermo- chemical process using downsized (ground) tire rubber particles (GTR) on a laboratory scale. An up scaled continuous process is currently under development. The up scaled process requires a calendering type machine to cool a flow devulcanized ground tire rubber (D-GTR) from an extruder. The development of this the cooling calender is described in this thesis.

The calender prototype has to be able to decrease the temperature of a D-GTR flow of 100 kg/hr from 250°C to 90°C. The cooling process should take place in an oxygen free environment to optimize the rubber quality. The calender will be rated to a minimum of 200 running hours and will have to be safe to operate. An initial budget of €5000, - was available for parts and materials. The realisation of the prototype was included during the project period.

The thermal and physical properties of D-GTR during a calendering process were determined from literature research. The properties were used as calculation input values in a parametric model. This model includes thermodynamical calculations and mechanical calculations of the various parts of the prototype. Laboratory testing is done as well, using a mixing mill. This was done to determine the necessary drive power of the calender and investigate milling behaviour of D-GTR. The parametric model was used during the design phase to define the basic machine parameters and dimensions.

An overview of possible design choices and configurations was made, and the final choices were made based on the calculations output and prototype requirements. The design choices were implemented into a 3D model of the prototype. Drawings of all machine parts were made for production. Some parts were outsourced and other parts were made in-house.

The finished design is a vertical, inclined three roller calender. The roller diameter is 250 mm and roller width is 200 mm. Heat is transferred from the D-GTR sheet to cooling water flowing through water channels near the roller surface. The required amount of heat which has to be cooled for the 100 kg/hr D-GTR flow is 8.2 kW.

The prototype has two compression stages, where D-GTR passes through a roller pair. Both nip heights are designed to be adjustable to prevent the formation of a bank before the nip. One drive motor is used to drive the three rollers. The motor will be controlled using a frequency converter making the rotational speed adjustable. The speed ratios between the rollers can be varied by changing the drive sprockets. The initial speed ratio is 1:1.1.

The machine, as displayed in this thesis has been built during the graduation period. The fabrication of safety covers and some final finishing still remains. Further testing will be done to verify the cooling properties, gas tightness and to check the performance of the prototype.

**CONTENTS**


---

Rubber recycling calender summary.....	2
contents.....	3
1 Introduction.....	6
1.1 tires.....	6
1.2 Tire waste and re-usage.....	7
1.3 Recycling by devulcanization .....	7
2 Background.....	9
2.1 Rubber recycling calender .....	9
2.2 Project goal.....	9
3 Literature review, with respect to material properties.....	10
3.1 Tire composition.....	10
3.2 Thermodynamical .....	11
3.3 Literature review concerning the calendering process.....	14
4 Cooling development.....	22
4.1 Parametric model theory.....	22
4.2 Thermodynamical calculations, 100 kg/hr flow of D-GTR.....	32
4.3 Roller design (cooling system).....	34
4.4 Results and discussion.....	37
5 Mechanical development .....	38
5.1 Calculations and general design .....	38
5.2 Results and discussion.....	54
6 Design specification.....	55
6.1 Total design.....	55
6.2 Material cost overview .....	57
7 Realisation.....	59
8 Conclusions and recommendations.....	62
8.1 Conclusions .....	62
8.2 Recommendations.....	63
9 Bibliography .....	65
Appendix 1, Plan of approach .....	72
1 Project background .....	75
1.1 Devulcanisation project.....	75
1.2 The graduation project.....	75
2 Project assignment and goals.....	76
2.1 Project description.....	76

2.2	Goals.....	77
3	Activities.....	78
3.1	Preparation and research phase.....	78
3.2	Concept phase .....	78
3.3	Realisation .....	79
3.4	Final phase.....	79
4	Project limits .....	80
4.1	Scope of the project.....	80
4.2	excluded of the project .....	80
5	Products .....	81
6	Quality assurance .....	82
7	Risk assessment .....	82
7.1	Planning and deadlines .....	82
7.2	Skills .....	82
7.3	Process changes.....	83
7.4	Parts delivery .....	83
7.5	Financial .....	83
8	Project organisation .....	84
9	Benefits and costs analysis.....	86
9.1	Costs .....	86
9.2	Benefits .....	86
10	Skills .....	87
11	Design specification.....	88
	Appendix 2, research reports.....	90
	Appendix 3, Calculations.....	93
1	Thermal calculations 100 kg/hr D-GTR.....	93
2	Bearing specifications.....	95
	Appendix 4, Part designs.....	58
1	Part specification .....	58



# 1 INTRODUCTION

## 1.1 TIRES

Modern car and truck tires are engineered to provide good durability, stability and traction between the wheels and the road, in a wide range of environments and conditions. Typical car tires consist of about 12 components, with specific functions for every component. The components are illustrated in Figure 1.

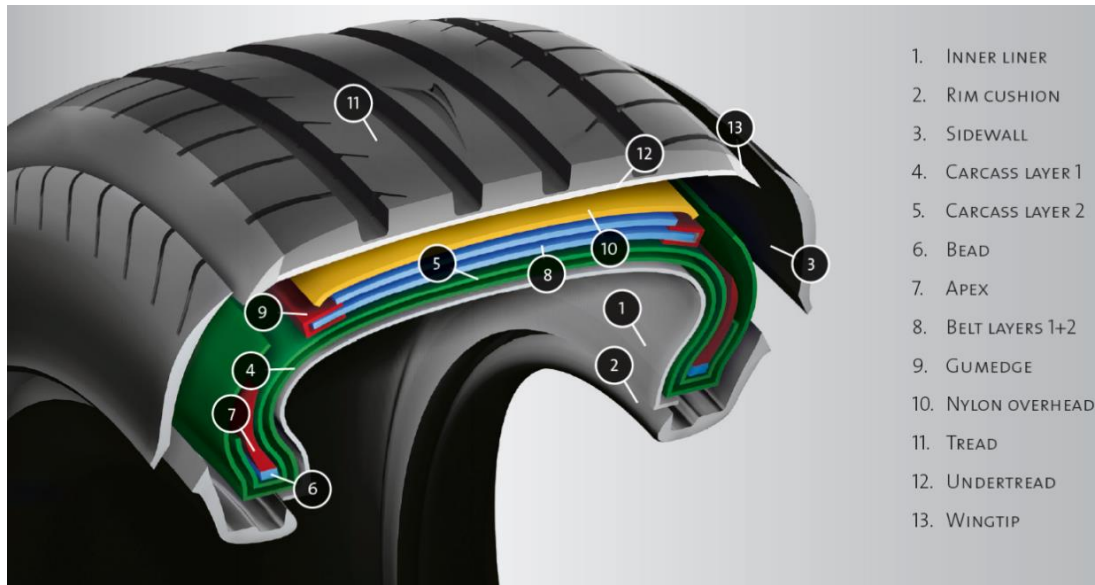


Figure 1, components of a car tire [19]

The largest mass fraction in a tire is rubber. Other fractions are fillers, textiles, metal wire and additives, as shown in

Table 1. The focus during this project is on car tires.

Tires are manufactured by stacking the components onto each other, then pressing them in a tire shape and curing them in moulds, using a process called vulcanization. The vulcanization process bonds the components together and converts the rubber into an elastic, insoluble and durable thermoset material. Other additives like stabilizers, anti-oxidants are used in tire production to ensure resilience against ageing and degradation by ozone, sunlight and high temperatures. This process offers great tire properties, but also creates challenges in waste tire processing and recycling.

Table 1, Composition of materials used in a tire, in percentages [1]

Type of tire	Car/passenger	Truck
Rubber/elastomer	41-48	41-45
Carbon black	22-28	20-28
Metal/steel	13-16	20-27
Textile	4-6	0-10
Additives	10-12	7-10

## 1.2 TIRE WASTE AND RE-USAGE

An estimated 17 million tonnes of discarded tires every year. The re-use of waste tires is done in several ways. The most energy- efficient way of re-using tires is retreading, which means vulcanisation of a new running surface on a used tire carcass. The casing of a tire hardly deteriorates during its first life. Retreading is common amongst truck tires, but not so much for car tires. This is partially caused by the relatively low costs of new car tyres and the fact that consumers put less trust into retreaded tyres. Approximately 9% of waste truck tires was retreaded in 2012. [1]

Tires of which the carcass is worn as well, can be recycled. 39% of waste tires were recycled in 2012. Products like mats, athletic tracks and asphalt are made using shredded tires. A considerably higher share of material recycling can be achieved if tire material can be used in a real recycling loop: tires back into tires. It is currently investigated how to create a process of converting waste car tire rubber into rubber compounds for new car tires. This project is part of that research.

Another way of using waste tires is by energy recovery, by using shredded tires as fuel, to produce heat. A percentage of 37% of all waste tires have been used for energy recovery in 2012. Tire rubber has a higher heat value than coal, 32.6 MJ/kg compared to 16.0-27.9 MJ/kg (depending of coal grade). The cement industry is one of the greatest waste tire consumers with tires being added to cement kilns as fuel.

## 1.3 RECYCLING BY DEVULCANIZATION

The most preferred way of recycling tires is to convert old tires into new tires. The challenge hereby is the material itself. Tires consist of various rubber compounds for the different components. A compound is a mixture of rubber polymer combined with fillers, processing aids, vulcanisation aids like sulphur and other additives.

The vulcanisation process consists of pressing the rubber compound in a mould, and subsequent cure at high temperatures. This converts the vulcanisation aids into sulphuric crosslinks ( $S_x$ ) between the polymeric rubber molecules as illustrated in Figure 2. This process creates a 3 dimensional network of rubber chains and crosslinks, which enhances the mechanical properties the rubber.

Devulcanization is a process which converts the vulcanised rubber into a state so it can be mixed, processed and vulcanised, using conventional processes. An ideal devulcanization process should only break the sulphuric crosslinks between the rubber chains, without chain scission of the rubber molecules themselves. A process with a large amount of scission of the polymer chains is called reclamation. This process deteriorates the quality and mechanical properties of the rubber.

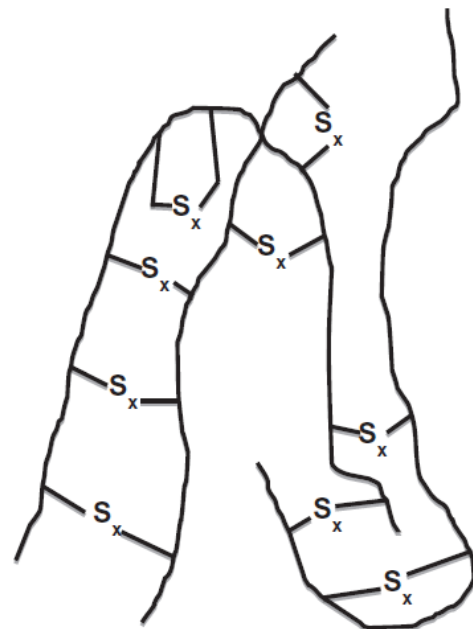


Figure 2, Schematic illustration of rubber molecule chains with crosslinks [1]

The University Of Twente, department of Elastomer Technology and Engineering (ETE) in cooperation with the University Of Applied Sciences Windesheim (professorship for Polymer Engineering) are currently conducting research in the field of rubber devulcanization process to enable recycling of car tire rubber. The method used is a thermo- chemical devulcanization method. Ground tire rubber (GTR) is mixed with devulcanization aids to break the sulphuric crosslinks, and prevent crosslinks to re-combine. GTR is downsized car tire rubber with particles up to 3.5mm. Non-rubber components like fibres and steel is removed out of the GTR.

The thermo- chemical devulcanization process is based on a laboratory scale batch process, developed and optimized by Sitisaiyidah Saiwari at the University of Twente [2]. The current investigation is to scale up from laboratory conditions to a semi- industrial scale. Hans van Hoek, PhD student at University of Twente and lecturer at the University of Applied Sciences Windesheim is developing and optimizing an up scaled continuous process using a twin-screw extruder for the devulcanization of GTR. This is based on the batch process by S. Saiwari.

## 2 BACKGROUND

The devulcanization process itself occurs inside the twin screw extruder. The D-GTR flow out the extruder will have a temperature of around 250°C. The extruder output has to be cooled to below 100°C to freeze the chemical reaction and to prevent sulphuric crosslinks to re-combine. The cooling process has to occur in an oxygen free environment to prevent oxidation of the D-GTR which may degrade the quality of the rubber.

### 2.1 RUBBER RECYCLING CALENDER

It is investigated that cooling with a calendaring process is economically most feasible and it improves product properties by adding additional shear. A schematic illustration of a calendaring process is shown in Figure 3. Calendaring is used to flatten and spread the devulcanizate to optimize the cooling capacity and enhance the surface quality. Direct contact of cooling water with D-GTR isn't allowed due to the irregular surface quality of the extruder output. For this reason, internal cooling will be implemented into the rollers.

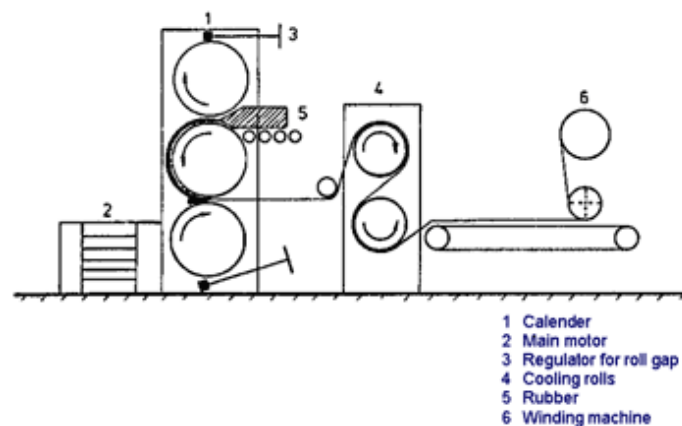


Figure 3, calendaring principle

### 2.2 PROJECT GOAL

The main goal of this project is to develop and realize a functioning calender to decrease the temperature of devulcanized rubber that leaves the extruder and to improve the surface quality and internal structure of the devulcanizate. It will be a calendaring type machine, to flatten the material, create a cooling surface and disperse internal heat. The machine will be classified as a working prototype. The initial required design specifications are

- Reducing a D-GTR flow of 100 kg/hr from 250°C to 90°C
- The cooling process has to occur in an oxygen free environment
- It should be safe to operate
- The prototype will be driven using 1 motor
- The prototype will be rated to 200 running hours

#### 2.2.1 Project Activities

- Understanding the behaviour of devulcanized rubber on a calender.
- Development of the cooling system (cooled rollers)
- Development of the mechanical part of the machine
- Building the prototype
- Testing the prototype

### 3 LITERATURE REVIEW, WITH RESPECT TO MATERIAL PROPERTIES

---

#### 3.1 TIRE COMPOSITION

A literature review has been done to understand the rubber properties. Therefore, we have to determine which materials are used in tire rubber, and the effects of the different materials on each other.

The thermal properties of tire rubbers are derived from literature. They depend on the composition of the tire. The kinds of rubbers and amount of fillers inside the compound determine the thermal properties. The composition of GTR may vary slightly from batch to batch. Car tires consist of several types of compounded rubber,

The composition of certain batch of devulcanized ground tire rubber (D-GTR) was analysed using a thermogravimetric analysis [2], Table 2. These values are indicative to the composition of the GTR.

*Table 2, Devulcanized GTR composition [2]*

Ingredient	%	phr
Polymers	46	100
Oils	12	26
Fillers		
- Carbon black	30	65
- Ash/mainly silica	12	26

Phr. is an abbreviation of “Parts per Hundred parts of Rubber polymer”. The rubber polymers in the composition adds up to 100 parts per hundred. In the D-GTR composition, the amount of carbon black filler was found to be 65 parts per 100 parts of rubber polymer. Another 26 phr consists other fillers, mainly silica.

The rubber polymers inside GTR is estimated to have an amount of 40 phr. SBR (Styrene-Butadiene Rubber), 30 phr. natural rubber, 20 phr. butadiene rubber and 10 phr. of Butyl- and halogenated butyl rubber. [2]

The amount of fillers inside a compound will affect the thermal properties. This is used as a factor to determine the thermal properties. More about this in paragraph 3.2.1 and 3.2.1.

The density of GTR is 1100 kg/m<sup>3</sup>.

### 3.2 THERMODYNAMICAL

To be able to calculate the thermodynamical specifications of the calender, it was necessary to have more insight into the thermal properties of GTR.

The properties of interest are

- specific heat capacity of rubber at constant pressure ( $c_p$ ) in [kJ/kgK]
- thermal diffusivity of rubber ( $k$ ) in [m<sup>2</sup>/s]
- thermal conductivity of rubber ( $\lambda$ ) in [W/mK]
- density of GTR ( $\rho$ ) in [kg/m<sup>3</sup>]

The correlation between the density, specific heat capacity, thermal conductivity and diffusivity is [3]:

$$k = \frac{\lambda}{\rho c_p} \rightarrow \lambda = k \rho c_p \quad (Eq. 1)$$

Equation 1 is used to calculate the thermal conductivity. The thermal diffusivity and specific heat capacity was derived from literature. As shown in equation 1, a linear relation was found between the conductivity and heat capacity, considering a constant diffusivity value.

#### 3.2.1 Thermal diffusivity

The diffusivity is common heat transfer analysis value. It indicates the time it takes for the temperature inside a sample of material to reach an equilibrium. It is a measure for the ability to conduct heat, relative to its ability to store heat. It is commonly measured using a ‘flash method’. [4] These measurements are done at constant pressure, this is why  $c_p$  is used.

Higher diffusivity values indicate that a material is more likely to transfer heat instead of storing heat as internal energy. In case of the cooling calender, a higher value of diffusivity allows better heat transfer, hereby reducing the necessary cooling surface. Several studies suggest values ranging from 0.09-0.29 x 10<sup>-6</sup> m<sup>2</sup>/s. These values vary according to the composition of the compound. [5] [6] [7]

Studies by Nasr [5] and Oleiwi [7] suggest that diffusivity rises with higher filler amounts of carbon black. This effect can be seen in Figure 4 and Figure 5.

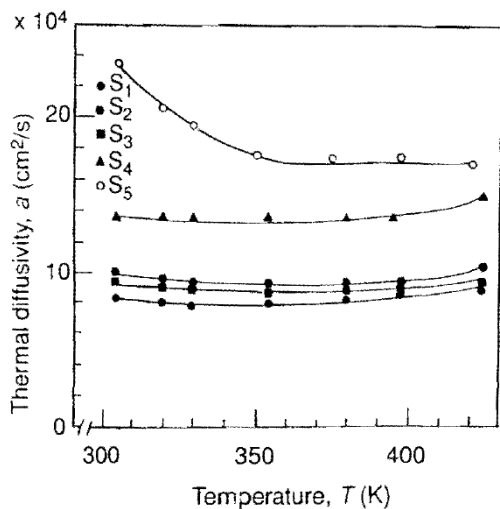


Figure 5, Thermal diffusivity of SBR + Carbon Black [5] (note: the values at the y-axis should be \*10<sup>-4</sup>!)

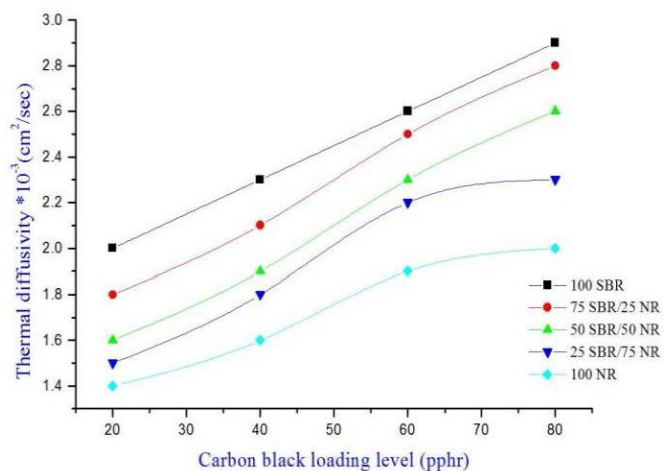


Figure 4, the influence of carbon black on diffusivity for SBR, NR and mixtures of SBR + NR [7]

In Figure 5, S1 is SBR without filler, and S2-S5 are samples with 30, 60, 80 and 100 Phr. carbon black filler.

The values in Figure 4, from the study of Oleiwi [7] are measured at room temperature ( $\approx 300\text{K}$ ). The values of both NR and SBR are considerably higher compared to the values measured by Nasr, ranging from  $0.14$  to  $0.29 \times 10^{-6} \text{ m}^2/\text{s}$  depending on the kind of rubber polymer and amount of filler.

Thermal properties of rubber with temperatures above  $160^\circ\text{C}$  are not studied much, because regular rubber processing requires lower temperatures compared to devulcanization. Nasr tested samples up to  $160^\circ\text{C}$ . The diffusivity plot as shown in Figure 5 indicates a relatively constant diffusivity value along the temperature range. Another study by Goyanes [6] using unfilled samples of SBR with NR showed a small decline of diffusivity along a range of  $300 - 400 \text{ K}$ . From  $0.1$  to  $0.08 \times 10^{-6} \text{ m}^2/\text{s}$ , concluding a relatively constant diffusivity along the temperature range.

The carbon black amount in D-GTR is 65 phr. The effect of 26 phr. of silica is not as significant as the effect of silica [8]. An amount of 65 phr. from Table 2 will be used as a reference for the thermal property values.

Using 65 phr. A thermal diffusivity value of  $0.10 \times 10^{-6} \text{ m}^2/\text{s}$  is taken from Figure 5, the graph in Figure 4 gives a value of  $0.23 \times 10^{-6} \text{ m}^2/\text{s}$  (using 50 SBR and 50 NR). A thermal diffusivity value of  $0.14 \times 10^{-6} \text{ m}^2/\text{s}$  is used during calculations, which is considered realistic.

### 3.2.2 Specific heat capacity of D-GTR

The specific heat capacity at constant pressure ( $c_p$ ) indicates the amount of thermal energy necessary to raise the temperature of a certain mass of material by  $1^\circ\text{C}$ . This value is used to calculate the amount of heat which has to be dispersed by the calender. The specific heat capacity is usually indicated in  $[\text{J}/\text{gK}]$  which equals to  $[\text{kJ}/\text{kgK}]$ .

The effect of a higher specific heat capacity value is a higher amount of internal energy, stored inside the rubber sheet. In case of the cooling calender, this means a higher flow of cooling water is necessary to reach a required temperature. It does not affect heat exchanging properties.

Multiple studies show that higher amounts of fillers inside the compounds tend to lower the specific heat capacity as illustrated in Figure 6. [9] [5]

The specific heat capacity rises with rising

temperature, as shown in figure 3. The rate of the heat capacity to rise, is almost equal for all filler grades, which seems to suggest that this effect is

caused by the rubber polymer. Multiple studies suggest that the specific heat capacity of carbon black filled rubber rises on a linear way, with rising temperatures.

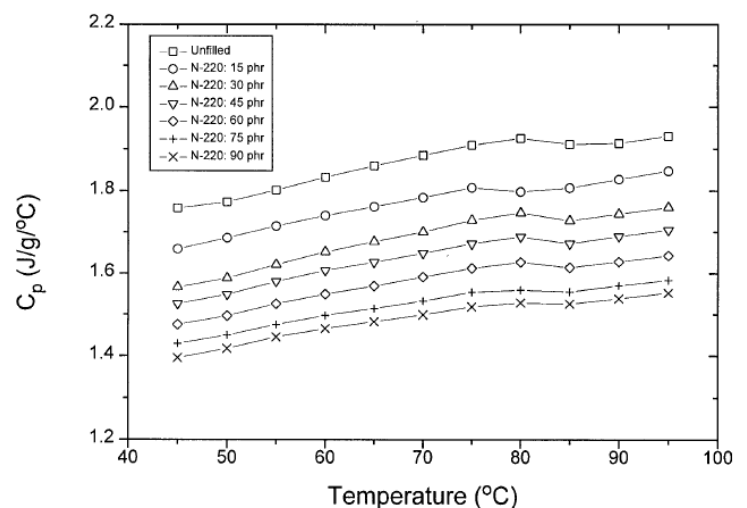


Figure 6, Specific heat capacity, depending on filler content and temperature (Natural rubber)

A mean specific heat capacity was used for calculation purposes, corresponding to a filler amount of approximately 65 phr. By using the change of  $c_p$  between 45- 95°C in Figure 6, a rise of 0.13 kJ/kgK is measured. This equals to  $2.6 \times 10^{-3}$  kJ/kgK per degree of temperature difference. The  $c_p$  value at 200°C will be used. This corresponds to  $c_p = 1.42 + (2.6 \times 10^{-3} \times 155) = 1.82 \text{ kJ/kgK}$

### 3.2.3 Specific heat capacity of cooling water

The temperature of the cooling water will be limited within a range of 20- 70°C to prevent condensation on the cooling roller surface at lower temperatures and to maintain a temperature difference between the D-GTR and cooling water at higher temperatures. The specific heat capacity of water almost doesn't change within this range [10]. The density will lower slightly with rising temperature, but this won't have a great effect. The mean specific heat capacity value is 4.18 kJ/kgK.

### 3.2.4 Thermal conductivity

Thermal conductivity is the ability of a substance to conduct heat from its warmer surface, to the colder surface.

The thermal conductivity is coupled to the thermal diffusivity and specific heat capacity as in equation 1.

The values from paragraph 3.2.1 and 3.2.2 are used to calculate the thermal conductivity, with a density value of 1100 kg/m<sup>3</sup>. The thermal conductivity as used in the calculations of this project is:

$$\lambda = k\rho c_p = 0,14 \times 10^{-6} \times 1100 \times 1,82 \times 10^3 = 0,28 \text{ W/mK}$$

### 3.2.5 Cooling conclusion

The thermal properties used in the calculations are summarized in Table 3.

*Table 3, thermal property values for calculations*

Thermal properties	Spec. Heat capacity	Diffusivity	Thermal conductivity	Density
value	1.82	$0.14 \times 10^{-7}$	0.28	1100
unit	kJ/kgK	m <sup>2</sup> /s	W/mK	kg/m <sup>3</sup>

These values are values corresponding to SBR with a fill grade of approximately 60 - 65 phr.

The exact diffusivity value of D-GTR using literature values is difficult to determine. It's expected to be within a range of 0.10 - 0.23 x 10<sup>-6</sup> m<sup>2</sup>/s. Diffusivity measurement of multiple D-GTR samples will be recommended to determine a more accurate value.

The specific heat capacity may vary as well. This doesn't affect heat exchanging properties, but may cause a change of the required cooling water flow to reach the desired temperature. An increase in specific heat capacity raises the amount of internal heat.

### 3.3 LITERATURE REVIEW CONCERNING THE CALENDERING PROCESS

Previous experiments by Saiwari [2] proved an improvement in D-GTR quality when a milling or calendering process was used after devulcanization. This was tested using a speed roller ratio of 1:1.13. Calendering operations are normally used to ensure an optimal sufficient surface quality for the production of flat rubber products like conveyor belts. Optimization of the surface quality is not the primary goal for the cooling calender.

The calendering process research was done by a literature research and practical experiments. Information was gathered from scientific articles to determine the calendering parameters and roller pressures. A lab scale mill was used for practical experiments to study D-GTR behaviour while milling, and to determine the power and necessary torque. The parameters necessary for the calender design are

- Nip pressure (literature)
- Speed ratio rollers (literature)
- Necessary torque and power (lab experiments)
- Rubber behaviour (lab experiments)
- Roller rotation speed (calculation)

The roller rotation speed varies according to the machine settings and mass flow from the extruder. This will be explained in chapter 5.

#### 3.3.1 Calendering pressure

D-GTR will be compressed between the rollers during calendering. The material entering the calender will form a bank, as shown in Figure 7. Mixing takes place inside the bank, which is not preferable for the cooling calender process. The bank height can be reduced by adjusting the nip height and rotational speed. Calendering reduces the thickness, and spreads the flow along the roller surface. The change of sheet width is hereby expected to be limited. The compression of D-GTR will cause radial pressures.

The rolling pressures are necessary to determine the radial forces on the roller. They are necessary to determine the strength of the rollers, bearings, and to dimension the entire machine. The unit for pressure, used during this project is MPa ( $\text{N}/\text{mm}^2$ ). The values in Figure 7 are indicated in Pa ( $\text{N}/\text{m}^2$ ).

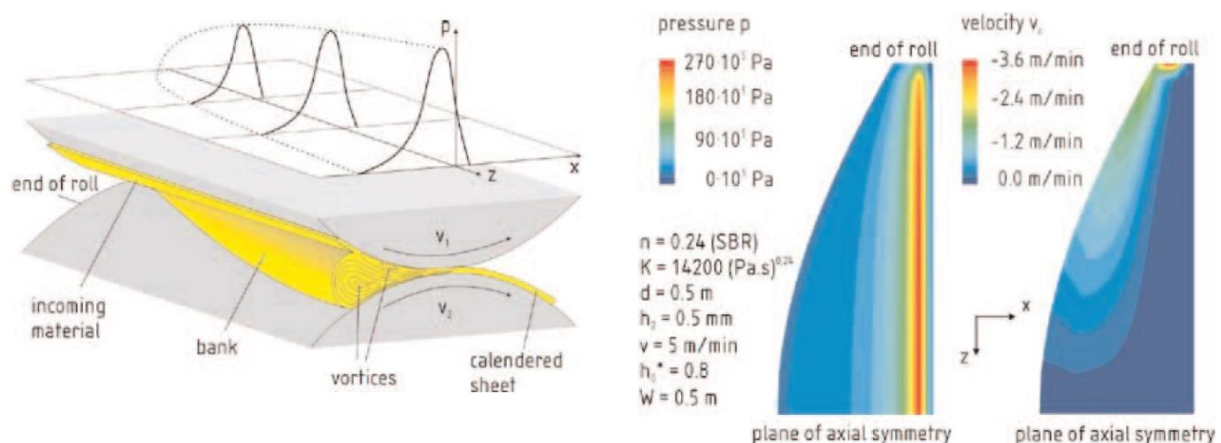


Figure 7, Calendering of material and pressure distribution graph

An analysis of calendering pressures of SBR rubber has been done by Luther and Mewes [11]. They used numerical lubrication equations to calculate, predict material flow, surface defects

and thermal effects of a rubber calendering process. The program used was Finite element software called Polyflow.

Their simulations give an indication for the roller pressures during calendering operations. The viscosity of D-GTR at room temperature is expected to be higher as a SBR compound, but lower than GTR. The calender has to handle D-GTR with a temperature ranging from 90- 250°C. Higher temperatures lower the viscosity and reduce calendering pressures. The viscosity of the SBR compound as simulated by Luther and Mewes is considered similar to hot D-GTR.

This change of viscosity makes it difficult to determine the exact calendering pressures. Roller pressure safety devices will be implemented into the design to prevent damage from unexpected rolling forces.

The cooling calender is designed to reduce the majority of the sheet thickness coming from the extruder in the first pass through the rollers. Multiple rollers may be used to create a sufficient surface area for heat transfer. Following roller pairs are designed for cooling purposes, large deformations are not expected.

The maximum rolling pressure should be within a certain operation window to optimize surface quality. A maximum pressure ( $p_{max}$ ) below 16 MPa is not ideal because of insufficient compression, which causes entrapment of air inside the sheet. On the other hand, the (peak) value of the pressure needs to be below 26 MPa, to prevent tearing and degradation of the rubber polymer.

The maximum pressure value, which will be used as an indication to calculate the roller pressure is determined to be  $22 \cdot 10^5$  Pa (22 MPa). The compression pressure is distributed in a parabolic way, as shown in Figure 7. The average pressure is determined to be  $(1/3) \cdot p_{max}$ .

$$p_{roller} = \frac{p_{max}}{3} = \frac{22}{3} = 7.33 \text{ Mpa}$$

A higher pressure causes more dissipation of mechanical energy into heat which is not preferable for the cooling calender. The roller pressure can be reduced by increasing the rotation ratio of the rollers and by increasing the nip height. This will reduce the radial roller pressure but increase shear inside the sheet.

During lab experiments, the sheet is found to be quite porous with air trapped inside. This decreases the density of the material, making it necessary to increase entrance speed of the calender. A density factor will be used during calculations to compensate for air pockets.

### 3.3.2 Speed ratio rollers

The rotational speed ratio, indicates the rotational speed difference between the rollers. One of the main effects of increasing the speed ratio is an increase in shear forces inside the sheet, which has the following effects:

- Improvement of D-GTR quality [2]
- Elimination of air bubbles inside the rubber sheet
- Reduction in radial pressure (to produce a certain sheet height)
- Forcing the sheet to switch to the faster turning roller

Beside calenders, mixing mills use speed ratios ranging from 1:1.1 to 1:1.25 for additional mixing. The mixing effect is not preferable for the cooling calender, to allow sampling in different stages during devulcanization.

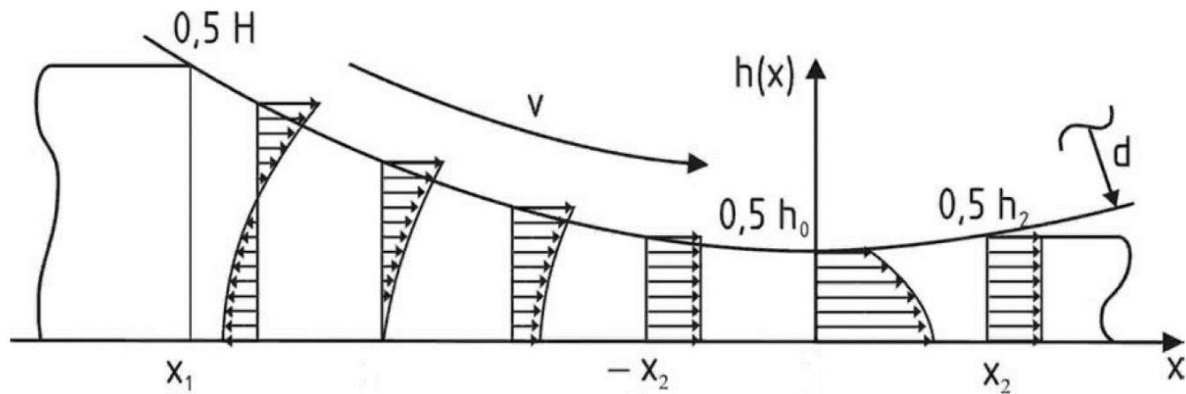


Figure 8, velocity profile between rollers with a speed ratio of 1:1 [12]

The speed ratio has an effect on the flow patterns inside the rubber sheet between the rollers. During milling, the rubber flow near the roller surface has a greater velocity than the material in the middle of the sheet (as in Figure 8). The velocity differences causes mixing and shear stress inside the bank and sheet. Increasing the speed ratio of the rollers tends to increase this effect even more

The operating window for the production of a 0.5mm thick sheet of SBR is shown in Figure 9. It shows the maximum pressure ( $P_{max}$ ) a function of the nip height ( $h_0$ ) and speed ratio of the rollers ( $f$ ). The grey band marks the optimal parameter window to produce a 0.5 mm sheet.

It shows that larger nip heights can be used, when the speed ratio is increased, thus reducing maximum pressure to reach a desired sheet height. This effect may be used in optimizing the calendering properties during the testing phase of the project.

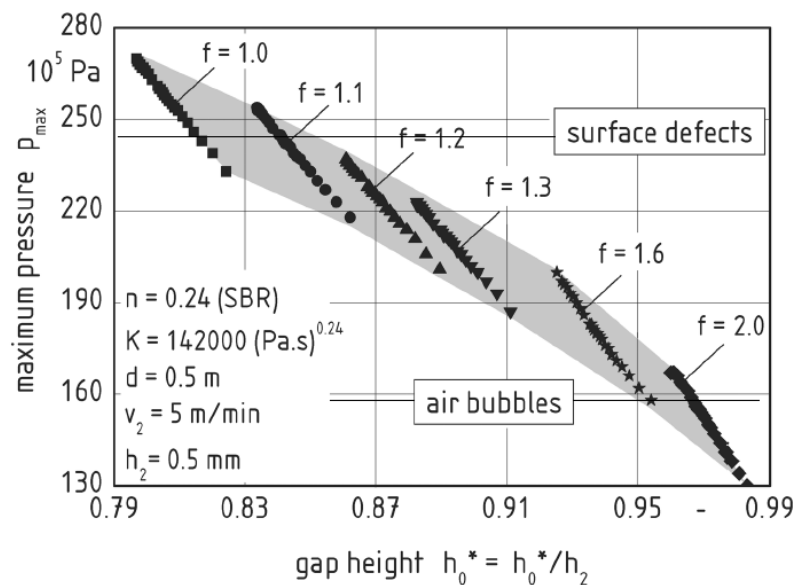


Figure 9, Calendering parameter window [11]

### 3.3.3 Cooling calender parameters

The roller pressure of 7.33 MPa, as determined in 3.3.1 will be used as a calculation value in determining the roller forces.

A speed ratio of 1:1.1 will be used in the first version of the devulcanization calender. This ratio is expected to eliminate air enclosure, while leaving the shear forces at a reasonable level. The design of the calender provides a possibility to change speed ratios by changing the sprockets which drive the rollers.

### 3.3.4 Laboratory experiments

Laboratory experiments were done using a laboratory size mixing mill. The goal of the experiment is to determine the torque and power to calender devulcanized GTR. Devulcanized batches were used during experiments. Unblended natural rubber at room temperature was used to clean the rollers.

The mixing mill is equipped with a current indication. The indicated current corresponds to the admitted power of the electric-motor. The mechanical and electrical losses are combined in a total efficiency  $\eta_{total}$ . The required power is calculated using equation 2

$$P_{req} = U_{in} \times (I_{load} - I_{idle}) \times \sqrt{3} \times \eta_{total} \quad (Eq. 2)$$

- $P_{req}$  is the required power in [W].
- $U_{in}$  is the 3-phase voltage in [V].
- $I_{load} - I_{idle}$  is the current difference between idle and high load indicated in [A].
- $\eta_{total}$  is the percentage of mechanical and electric losses.

The calculated power was used to calculate the required torque, using the following equation

$$T = \frac{P_d \times s_f}{2\pi n} \quad (Eq. 3)$$

- $T$  is torque in [Nm],
- $s_f$  is a safety factor and
- $n$  is the rotational speed in [Rev/s].

The max torque will be used as a design value.

### Equipment

The equipment used during the experiments:

- Mixing mill,
  - o Schwabenthan
  - o Type: ASC1
  - o Roller diameter: 80 mm
- Mixer
  - o Brabender Plasticorder 350S

### Procedure

Three batches of GTR were weighed according a certain filling degree of the mixer. The batches were mixed and heated during a 10 minute period using the Brabender mixer, hereby devulcanizing the GTR. The temperature and torque of the mixer were plotted during mixing. After this time, the mixer was emptied and the devulcanized GTR was transported to the mixing mill.

The mixing mill is pre-set to certain parameters. The main milling parameters were:

- Rotation speed of the rollers [RPM]
- Nip height [mm]
- Speed ratio [1 : 1.13]

The parameters were noted in Table 4. Other rubber behaviour observations were noted as well, and described. The complete dataset can be found in appendix 2.

**Results and conclusions**

Three batches were devulcanized. The mixing parameters are summarized in Table 4.

*Table 4, mixing parameters*

Mixing parameters	Mixer [RPM]	Fill grade [%]	mixing time [min]	temperature rubber start [°C]	Temp. After mixing [°C]
<b>1st batch</b>	150	62	10	60	185
<b>2nd batch</b>	150	70	10	<60	206
<b>3rd batch</b>	200	70	10	<60	231

Differences in material properties were noticed between the different batches. The first batch was mixed at a low fill grade of 62%. As a result, the temperature did not rise above 180°C for 10 min. The result was a granular consistency shown in Figure 10. The other two batches were mixed with fill grades of 70%. These did reach the desired temperature for devulcanization and had a smoother consistency as in

*Figure 10, not smooth on the mill (first batch)*



The consistency has a great effect on milling behaviour. The first batch stuck more to the surface of the roller and did not form a smooth sheet of rubber. Batches 2 and 3 stuck less to the roller and formed a uniform sheet, which accumulated on the faster turning roller as in Figure 12.

Table 5, milling parameters

Mixing parameters	Mixer [RPM]	Fill grade [%]	mixing time [min]
1st batch	150	62	10
2nd batch	150	70	10
3rd batch	200	70	10

Table 6, milling parameters (continuation)

Milling experiments	Nip height [mm]	Roller [RPM]	current idle [A]	Current load [A]	consistency	milling behaviour	Rubber sticks to 1 roller?	Removable from rollers?
1st batch	1	11	2.3	2.5	not smooth	poor	no	difficult
2nd batch	0,5/0,7	11	2.3	2.5	smooth	good	yes	yes
3rd batch	0,9	26	2.3	2.8	smooth	good	yes	yes

Table 5 and Table 6 gives an overview of the main milling parameters and observations. The noted amperages are used to calculate the required torque.

### 3.3.5 Lab mill power and torque calculation

The currents of the 3<sup>rd</sup> batch (Table 6) are used to determine the required power. It is calculated using equation 2.

The mechanical and electrical losses were determined at 49%. Using the values of Table 5, the delivered power is.

$$P_d = 400 \times (2.8 - 2.3) \times \sqrt{3} \times 0,49 = 170 \text{ W}$$

The calculated power, corresponds to a roller speed of 26 RPM. The torque was calculated using equation 3

$$T = \frac{P_d}{2\pi n} = \frac{170}{2\pi \times \left(\frac{26}{60}\right)}$$

Using the parameters of the 2<sup>nd</sup> batch in equation 3, a torque value of 59 Nm was found. Which is relatively close to the torque of the 3<sup>rd</sup> batch, concluding that the required torque remains relatively constant with various rotational speeds.

The calculated torque is valid for the mixing mill used during the lab experiments. It has a roller diameter of 80 mm. The required torque is expected to be different using other roller diameters. The tangential force ( $F_{tan}$ ) during milling or calendaring is expected to be constant. This assumption is illustrated in

Figure 12



Figure 11, Milling of devulcanized rubber

$F_{tan}$  is used to determine the required torque to drive a roller pair of a certain diameter. The torque can be calculated using

$$T = F_{tan} \times R \quad (Eq. 4)$$

- R is the roller radius in [m]

The tangential force, using a safety factor  $s_f$  of 2, to ensure sufficient power is

$$F_{tan} = \frac{T \times s_f}{R} = \frac{63 \times 2}{0.08/2} = 3117 \text{ N}$$

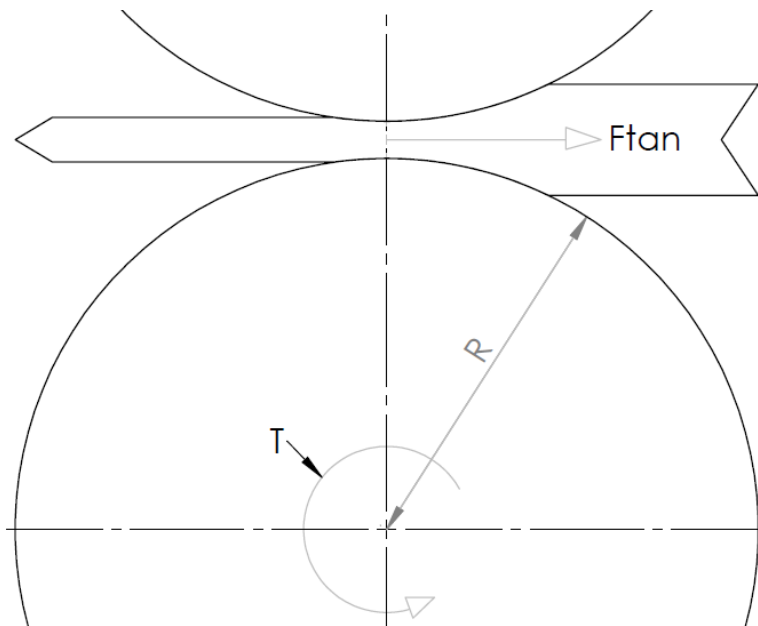


Figure 12, Tangential force

The calculated tangential force of 3117 N is used as an input value to further develop the transmission.

### 3.3.6 Mechanical conclusions

A calendering pressure of 7.33 MPa is used in bearings, shafts and frame calculations.

A tangential force of 3117 N was determined, using the roller diameter of 80 mm and a safety factor of 2. This value, along with the roller pressure, will determine the specifications of the transmission parts.

Table 7, mechanical input values

Property	Value	unit
Radial pressure roller	7.33	Mpa
Speed ratio rollers	1: 1.1	
Tangential rolling force	3117	N

Table 7 gives an overview of the first parameters of the machine, as derived from the calculations and experiments. These values, derived from both experiments and literature, have given an insight in the expected load during calendering. Safety factors and overpressure safeties will be included into the design to further compensate for any inaccurate assumptions.

The sticky behaviour of some batches of D-GTR, is an issue that may be resolved by using scraping devices, and by applying an anti-stick coating on the roller surface. A second function of the scrapers is to prevent material from re-entering the nip, hereby preventing a build-up of D-GTR before the nip.

As observed from the lab experiments, the input width is expected to spread to about double the width at the output. The sheet thickness after the nip is estimated to be about double the height of the nip. These assumptions are used in surface calculations. The exact rate of expansion is yet to be investigated.

## 4 COOLING DEVELOPMENT

---

The main components that provide cooling are the cooling rollers, where heat transfer between the GTR and cooling water occurs. The goal of this chapter is to determine the optimal heat transfer between the cooling water and devulcanized rubber. The roller surface is where the rubber is spread and heat transfer occurs. To dimension the cooling rollers, the following activities are done:

- Calculation of the amount of heat dispersed in the calender.
- Roller diameter and number of rollers.
- Heat transfer calculations
- Designing the rollers

Thermodynamical calculations were used to calculate the cooling capacity of the machine. The heat content of the rubber flow and the amount of heat which can be exchanged between the cooling water and rubber (heat flux) are required input to design the rollers. The calculations are performed in two steps.

- The thermal input and balance
- Heat transfer calculations

A parametric model is made for all mechanical and cooling calculations. The underlying theory is explained in chapter 5.1. The calender should be able to cool down a mass flow of rubber from the extruder of 100 kg/hr, from a temperature of 250 to 90°C, using indirect cooling with water. These values will be inserted in the parametric model and the output will be analysed and explained in chapter 5.2. The output is used to create a design specification of the machine.

The thermal and mechanical values from Table 3 and Table 7 are used as input and calculation values in the parametric model.

### 4.1 PARAMETRIC MODEL THEORY

#### 4.1.1 Thermal input and balance

The heat content is the amount of thermal energy inside the material. The amount of heat which has to be transferred from the GTR to the cooling water, is calculated using the known and desired temperature of the rubber and cooling water. The amount of heat is calculated using equation 4.

$$\dot{Q} = \dot{m} \times c_p \times \Delta T \quad (\text{Eq. 5})$$

- $\dot{Q}$  is the amount of heat expressed in [J/s] which equals to [W]
- $c_p$  is the heat capacity of the devulcanized rubber [kJ/kgK]
- $\Delta T$  is the temperature difference between the output of the extruder and the output of the cooling calender in [K].
- $\dot{m}$  is the mass flow of either D-GTR or cooling water expressed in [kg/s]

Equation 5 is used for both the D-GTR and the cooling water flow. For the latter, the heat capacity of vulcanised rubber is substituted by the heat capacity of water.

The heat balance is illustrated in Figure 13. The left side illustrates the rubber side and the cooling water is on the right.

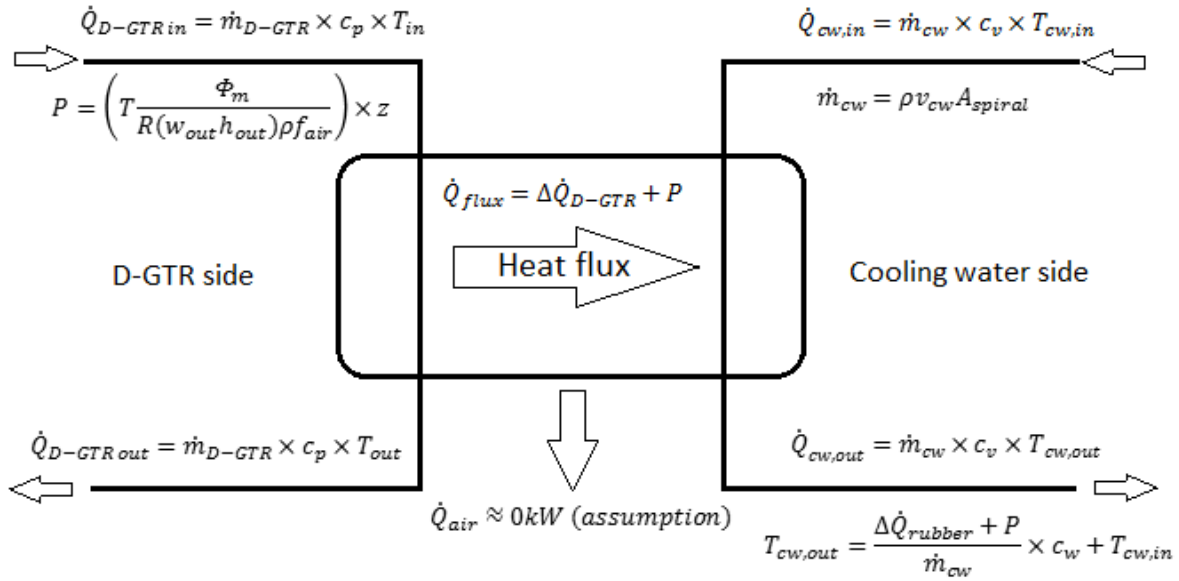


Figure 13, Thermal balance calender

The cooling process is considered a steady state situation, because there is a constant rubber supply, containing a certain amount of heat. A constant flow of heat enters, and flows out of the machine. The total amount of heat entering the machine has to be equal to the amount of the flowing out of the machine.

$$\dot{Q}_{in} + W_{in} = \dot{Q}_{out} \quad (Eq.6)$$

The heat flux is the flow of heat, exchanged between the hot D-GTR and cooling water. Besides thermal energy, mechanical energy is used to flatten the rubber. The mechanical energy is transformed into heat during the deformation of the material. This amount is added to the thermal energy of the rubber. The calculation of mechanical energy is explained in the following paragraph.

#### 4.1.2 Rubber flow, rotational speed and power input

The mechanical energy equals the amount of power necessary to drive the rollers. The torque is determined using equation 4 and depends on the roller diameter. The drive power, used to drive the roller is specified by the following equation

$$T = \frac{P}{2\pi n} = \frac{P}{\omega} \quad [Nm] \quad (Eq.7)$$

- $T$  is torque in Nm
- $P$  is power in [W]
- $n$  is the number of revolutions per second in [rev/s]
- $\omega$  is the rotational speed in [rad/s]

The rotation speed of the calender rollers depends on the mass flow, height and width of the calendered sheet. The mass flow is specified in [kg/s]. It equals to the volume flow  $\dot{V}_{D-GTR}$  in [m<sup>3</sup>/s] multiplied with the density  $\rho$  [kg/m<sup>3</sup>]:

$$\dot{m}_{D-GTR} = \dot{V}_{D-GTR} f_{air} \rho$$

$f_{air}$  is a factor to compensate for the air inside the D-GTR flowing out of the extruder. The density of air is low, thereby increasing the volume flow passing through the rollers.

The velocity of the rubber sheet is calculated by splitting the volume flow into a sheet velocity  $v_{out}$  [m/s] and the calendered sheet surface  $A_{out}$  [m<sup>2</sup>]. The surface is comprised of the sheet width and height.

$$\dot{m}_{D-GTR} = v_{out}(w_{out}h_{out})\rho f_{air}$$

The output thickness is estimated to be the nip height  $\times 200\%$ . This is caused by expansion of the rubber sheet after the nip. This expansion is observed during the lab experiments.

A calendering process with the mentioned parameters from the equation is shown in Figure 14. The width, height and velocity vary according to the machine settings and the amount of extruded rubber.

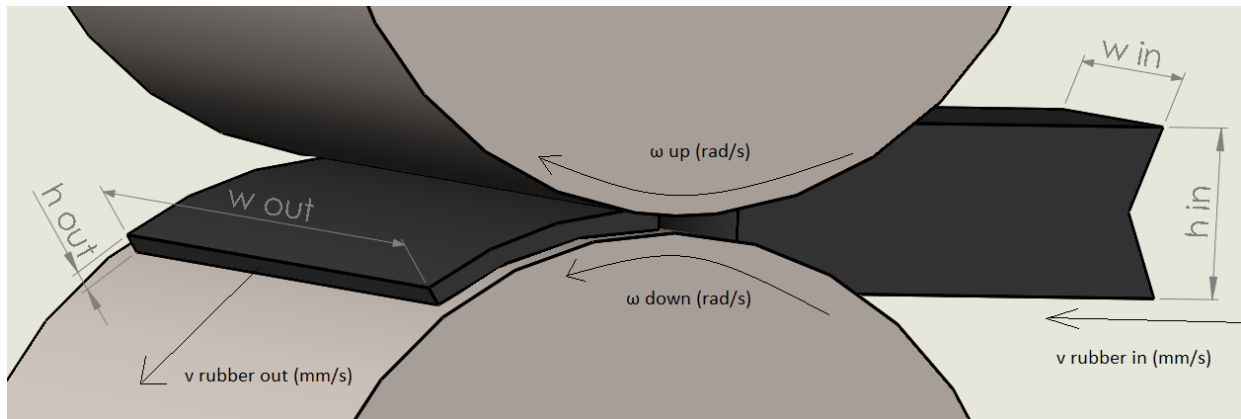


Figure 14, calendering schematic view

The sheet velocity is used to calculate the rotational speed of the roller.

$$\dot{m}_{D-GTR} = v_{out}(w_{out}h_{out})\rho f_{air} \rightarrow v_{out} = \frac{\dot{m}_{D-GTR}}{(w_{out}h_{out})\rho f_{air}} \quad (Eq. 8)$$

The line speed  $v_{out}$  equals the circumference speed of the roller, hereby assuming there's no slip between the rubber sheet and the roller surface. The rotary speed is calculated using

$$v_{out} = R\omega \rightarrow \omega = \frac{v_{out}}{R} \quad (Eq. 9)$$

Equations 6, 7 and 8 are combined to get a useful equation for the parametric model leading to the following equation for 1 roller pair.

$$P_{roller\ pair} = T \times \omega \rightarrow T \frac{v_{out}}{R} \rightarrow T \frac{\dot{m}_{D-GTR}}{(w_{out}h_{out})\rho R} = T \frac{\dot{m}_{D-GTR}}{(w_{out}h_{out})\rho R} [W] \quad (Eq. 10)$$

- T is the torque in [Nm] from Table 7.
- $\dot{m}_{D-GTR}$  is the mass flow of devulcanized rubber [kg/s],
- $\rho$  is the density of D-GTR from Table 3 in [kg/m<sup>3</sup>].
- R is the radius of the calender roller in [m].

$R$ ,  $w_{out}$  and  $h_{out}$  are values depending on the design and configuration of the machine. These values are chosen manually, keeping the maximum distribution in width in mind, as mentioned in paragraph 3.3.6.

Multiple rollers are used to create a sufficiently large cooling area. The total required drive power is calculated using:

$$P_{motor} = \frac{P_{roller\ pair} \times z}{\eta_{mech}} \quad (Eq. 11)$$

- $P_{motor}$  is the required motor power
- $z$  is the number of roller pairs
- $\eta_{mech}$  is the percentage of total mechanical loss of the transmission.

The drive power is considered equal for all roller stages. The roller pressures of the different stages may vary. The thermal input, created by rubber deformation equals to the drive power, without the mechanical losses.

#### 4.1.3 Logarithmic temperature difference

The temperature difference, used in the heat transfer equation is a logarithmic mean temperature difference. It specifies the average temperature difference between the (hot) rubber and (cold) cooling water. The cooling water spirals through the roller, thereby assuming 'counter flow' conditions.

The following equation is used.

$$\Delta T_{lnCF} = \frac{(T_{H,out} - T_{C,in}) - (T_{H,in} - T_{C,out})}{\ln\left(\frac{T_{H,out} - T_{C,in}}{T_{H,in} - T_{C,out}}\right)} \quad (Eq. 12)$$

- $T_H$  is the temperature of the rubber
- $T_C$  is the cooling water temperature.

The D-GTR temperatures are 250°C at the inlet and 90°C at the outlet, as described in the project goals. The cooling water inlet temperature is 30°C. The cooling water outlet temperature depends on the cooling water flow, and the heat flux. It can be calculated by

$$T_{cw,out} = \frac{\dot{Q}_{flux}}{\dot{m}_{cw}} \times c_v + T_{cw,in} \quad (Eq. 13)$$

- $T_{cw,out}$  is the cooling water outlet temperature
- $T_{cw,in}$  is the cooling water inlet temperature
- $\dot{m}_{cw}$  is the mass flow of cooling water in [kg/s].
- $c_v$  is The specific heat capacity at a constant volume

#### 4.1.4 Heat transfer

Rollers with internal cooling will be used to cool the D-GTR. Heat exchange calculations are carried out to determine the necessary cooling surface and cooling water flow. The necessary data for these calculations:

- Thermal and flow properties of water
  - o Viscosity
  - o Specific heat capacity ( $c_{water}$ )
- Thermal properties of the roller surface
  - o Wall thickness
  - o Thermal conductivity of the roller material

The heat flux ( $\dot{Q}_{flux}$ ) between the rubber and cooling water is determined using the desired temperature values of the D-GTR. The heat flux is used in further heat transfer calculation to dimension the machine. It is calculated by adding the mechanical dissipation of energy ( $\dot{W}_{in}$ ) to the required heat to cool the D-GTR ( $\Delta\dot{Q}_{D-GTR}$ ).

$$\dot{Q}_{flux,req} = \Delta\dot{Q}_{D-GTR} + \dot{W}_{in} [W] \quad (Eq. 11)$$

The available heat flux depends on the design of the machine. The heat flux is determined by.

$$\dot{Q}_{flux,av} = K \times A$$

$\Delta T_{lnCF}$  is the logarithmic mean temperature difference of the D-GTR in [°C]. K is the heat transfer coefficient in [W/m<sup>2</sup>K] and A is the cooling surface area in [m].

The heat transfer coefficient indicates the heat transfer rate between the hot rubber and cooling water. It is a comprised value, combining the convection of the cooling water to the wall, conduction value of the roller wall and conduction of the rubber itself. The heat transfer coefficient is calculated using the following equation

$$K = \frac{1}{\left(\frac{1}{\alpha_{cw}} + \frac{D_{roller}}{\lambda_{roller}} + \frac{D_{D-GTR}}{\lambda_{D-GTR}}\right)} \left[\frac{W}{m^2K}\right] \quad (Eq. 13)$$

K is the heat transfer coefficient [W/m<sup>2</sup>K],  $\alpha_{cw}$  is the convection value of the cooling water in [W/m<sup>2</sup>K],  $D_{roller}$  is the wall thickness between the cooling water and roller surface [m],  $\lambda_{roller}$  is the thermal conductivity value of the roller material [W/mK],  $D_{D-GTR}$  is the sheet thickness of the rubber [m] and  $\lambda_{D-GTR}$  is the thermal conductivity of the rubber [W/mK]. The values from the paragraph 3.2.5 are used here.

#### 4.1.5 Convection

The rollers are designed with cooling channels near the roller surface to optimize heat transfer. The rate of heat transfer between the cooling water and the roller wall is described by the convection value ( $\alpha_{cw}$ ). This value is determined using convection equations. It depends on several factors such as the flow properties of the liquid, shape of the flow channel, viscosity, specific heat capacity and thermal conductivity.

The convection value is calculated using the dimensionless numbers, Reynolds (Re), Prandtl (Pr) and Nusselt (Nu). These dimensionless numbers describe the flow and heat transfer properties, and will be used in a parametric model to calculate the convection value. The necessary input data were:

Cooling water properties [10]

- |                                  |                        |
|----------------------------------|------------------------|
| - Dynamic viscosity $\mu$        | 8.00E-04 pa s          |
| - Density $\rho$                 | 1000 kg/m <sup>3</sup> |
| - Spec. heat capacity $c_p$      | 4.18 kJ/kgK            |
| - Thermal conductivity $\lambda$ | 0.580 W/mK             |

Depending of the design

- Velocity at roller surface  $v$
- Hydraulic diameter cooling water channel  $D$

The velocity ( $v$ ) and hydraulic diameter ( $D$ ) function as adjustable parameters during the design process. The other values correspond to the thermal and flow properties of water, derived from literature. [10]

The equations used to calculate the convection value:

$$Pr = \frac{c_p \mu}{\lambda} \quad (Eq. 14) \qquad Re = \frac{\rho v D}{\mu} \quad (Eq. 15) \qquad Nu = \frac{\alpha D}{\lambda} \rightarrow \alpha = \frac{Nu \times \lambda}{D} \quad (Eq. 16)$$

Reynolds (Re) describes the flow properties of the cooling water in the roller. A Reynolds number above 2600 indicates a turbulent flow, which has a positive effect on heat exchange properties.

The Prandtl number describes the ratio of diffusivity. The Prandtl number, along with the Reynolds number will be used to calculate  $\alpha_{cw}$

The Nusselt number describes the ratio between the convective and conductive heat transfer on the boundary between a solid and a fluid. The relation between Nu, Re and Pr is described by Dittus and Boelter [13] which is valid with a turbulent flow with  $Re > 10000$  and Prandtl numbers in the range of 0.7 – 100.

$$Nu = 0,023 Re^{0,8} Pr^{0,33} \quad (Eq. 17)$$

The convection value is calculated using the Nusselt number.

#### 4.1.6 Surface area and sheet thickness

The Surface area ( $A$ ) is the area of contact between the D-GTR and the rollers, expressed in  $[m^2]$ . A larger surface area creates a higher rate of heat exchange, as in equation 12.

$$\dot{Q}_{flux,av} = K \times A \times \Delta T_{lnCF} [W]$$

The surface area is calculated using a cross-section of the rollers, and drawing a sheet on the rollers as in Figure 15 (next page). The arc lengths  $l_1$ - $l_4$ ,  $l$  bottom and  $l$  middle are the areas where D-GTR contacts the roller surface. The surface area depends on the following factors

- Roller diameter
- Amount of rollers
- Roller angles
- Nip height
- Sheet thickness

These factors for the calculations of the arc lengths. The surface width is not equal on all rollers. The first stages flattens the sheet to about the required sheet thickness, and spread the sheet along the width of the rollers.

The surface areas can be divided in 2 kinds of areas. The surfaces between the nips, where the sheet is flattened, spread and cooled between two surfaces ( $l_1 + l_2$  and  $l_3 + l_4$ ), and areas on the roller surface where the sheet is cooled on one side ( $l$  bottom,  $l$  middle).

Each area has different sheet heights and widths. The width of the sheet on the middle roller is considered an input value. It will not have an unlimited width because the extruder output is only 40 mm wide.

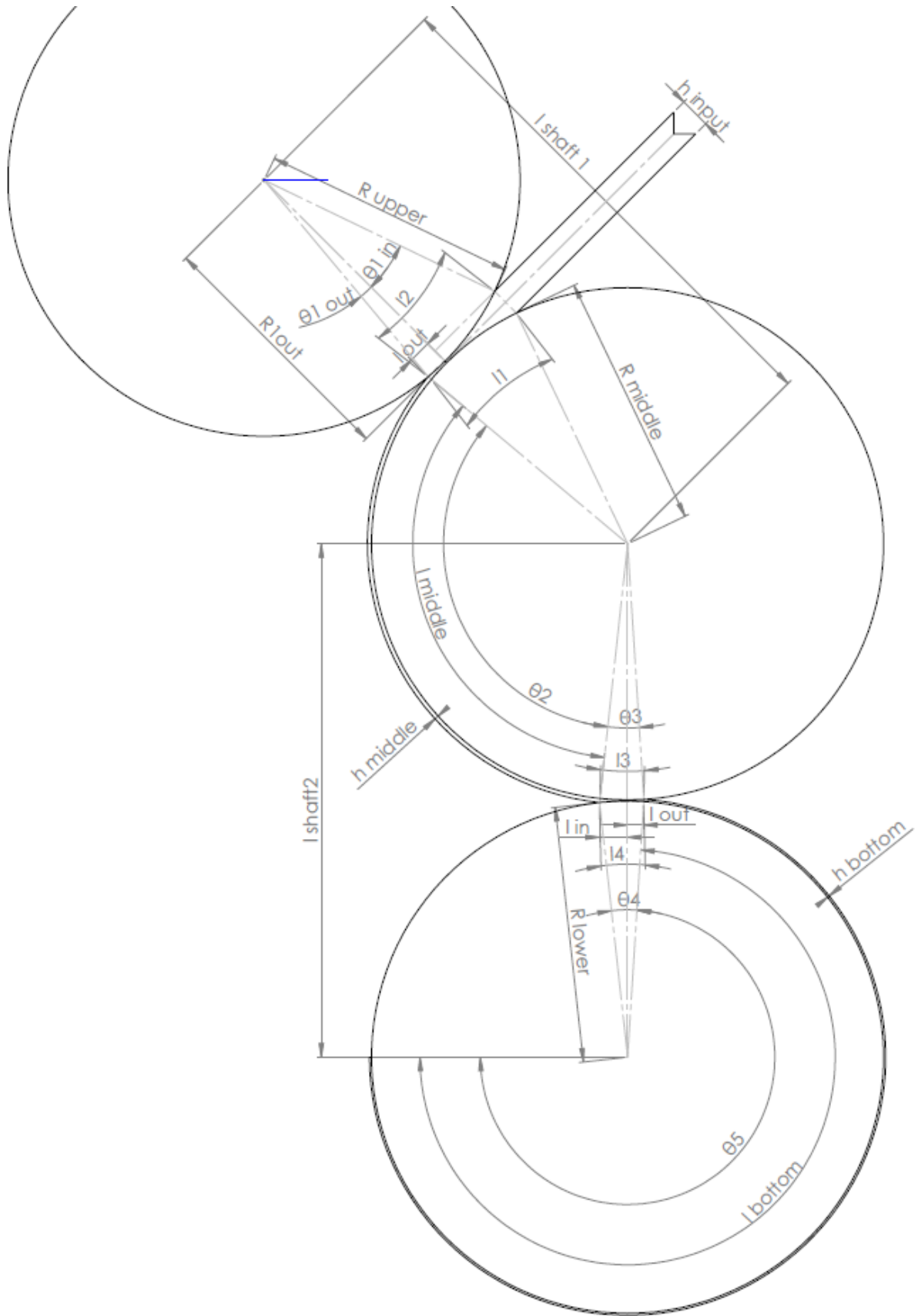


Figure 15, Surface calculations

The sheet thickness varies along the calender surface. It depends on the nip heights, input height and output height at the nip. The nip heights depend on the settings of the calender. The sheet width increases when the nip height is decreased.

Equation 13 shows that a decrease in sheet thickness has a great influence on the heat transfer coefficient value. D-GTR has a low thermal conductivity and a decrease of  $D_{rubber}$  in the following equation, this leads to a strong increase of the K value.

$$K = \frac{1}{\left(\frac{1}{\alpha_{cw}} + \frac{D_{roller}}{\lambda_{roller}} + \frac{D_{D-GTR}}{\lambda_{D-GTR}}\right)} \left[ \frac{W}{m^2K} \right]$$

The effective sheet thickness, necessary for heat exchange calculations, varies between the rollers, because the sheet contacts the roller on 2 sides. The mean sheet thickness between the nip ( $h'$ ) is calculated using the nip height, sheet height and inlet height, each corresponding to a certain arc length.

$$(h') = \frac{(h_{in} + h_{nip}) \times \left(\frac{l_{nip \rightarrow in}}{l_1}\right) + (h_{out} + h_{nip}) \times \left(\frac{l_{nip \rightarrow out}}{l_1}\right)}{2} \quad (Eq. 20)$$

The D-GTR between the rollers is cooled from two sides. This is why  $h'/2$  is used there, resulting in the following equation for the heat transfer coefficient between the nip

$$K_{nip} = \frac{1}{\left(\frac{1}{\alpha_{cw}} + \frac{D_{roller}}{\lambda_{roller}} + \frac{h'/2}{\lambda_{D-GTR}}\right)} \left[ \frac{W}{m^2K} \right] \quad (Eq. 21)$$

**4.1.7 Machine configuration (rollers and cooling)**

The first design were the roller dimensions, amount of rollers, and calender shape. These choices were necessary to determine the calendering power, and allow for further mechanical calculations.

Using the surface area calculations (4.1.6) and heat transfer equations, the necessary surface area and amount of rollers were determined. The necessary amount of rollers is 3. They will be in an inclined 3-roll calender configuration as in Figure 16. The inclined upper roller ensures easy feeding of extruded rubber. The calender will be installed with the upper rollers just below the extruder nozzle, so extruded rubber will simply drop between the rollers of the calender.

Inclined Form :

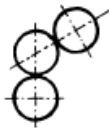


Figure 16, inclined 3 roll configuration

The rubber sheet is cooled on 2 sides when a 3 roller calender is used. The rubber sheet switches side between the middle and bottom roller (as in Figure 18). By switching the sheet to another roller, the hot side will come into contact with the 3<sup>rd</sup> roller, thereby raising the temperature difference and improving the cooling capacity. Rubber does not have a great thermal diffusivity, so it is expected that after a period of contact with the roller, one side of the sheet will be cooler than the opposite side of the sheet.

Regular calender rollers are quite wide compared to their diameter, like the calender in Figure 19. This is ideal for creating wider sheets, or textile production, but not necessary for cooling purposes. Advantages of larger diameters

- Expanding the surface area
- Surface between nip is larger (double sided cooling)
- Decrease in rotational speed of the rollers.

A positive effect of limiting the width of the rollers is a reduction of bending forces, caused by the nip pressure. This ensures lighter construction, thereby reducing material costs. The chosen roller dimensions became:

Table 8, roller specifications

Property	Value	unit
number of rollers	3	
Roller diameter	250	mm
Roller surface width	200	mm

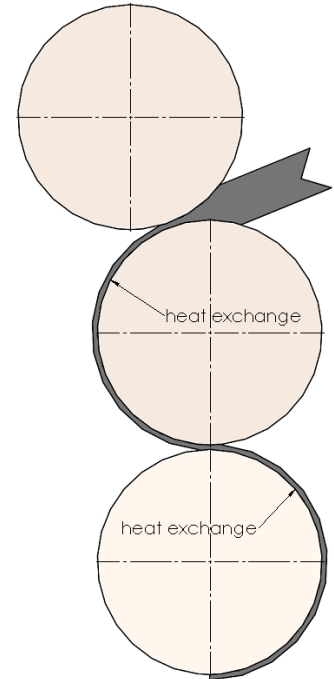


Figure 17, Rubber flow on calender



Figure 18, regular laboratory calender

## 4.2 THERMODYNAMICAL CALCULATIONS, 100 KG/HR FLOW OF D-GTR.

The requirements of the machine were established at the beginning of this project. The main requirement is to cool a flow of 100 kg/hr of devulcanized rubber, from 250°C to 90°C. The goal of the calculations is to determine the basic design parameters to cool this flow of D-GTR. The most important value to determine is the available heat flux. This is the amount of heat the machine is able to extract from the D-GTR flow in [W]. The available heat flux has to be equal to the required heat flux to reach 90°C.

Table 9, input parameters 100 kg/hr

<b>Parametric calculation values</b>			
<b>Property</b>	<b>value</b>	<b>unit</b>	<b>remarks</b>
<b>Input values D-GTR</b>			
Mass flow D-GTR	100	kg/hr	
Density D-GTR	1100	kg/m <sup>3</sup>	
Air fraction D-GTR	0,9		
Temperature rubber in	250	°C	
Temperature rubber out	90	°C	
Extruder output cross section	996,13	mm <sup>2</sup>	
<b>Machine parameters</b>			
Amount of roller pairs	2		
Roller diameter	0,25	m	
Roller width	0,2	m	
Rubber sheet width 1st stage	80	mm	
Nip height 1st stage	1,3	mm	
Nip height 2nd stage	0,5	mm	
Cooling spiral diameter	0,01	m	
Channel spiral hydr.D	0,005	m	Half circle
Velocity waterflow v (spiral)	4	m/s	
Incline upper roller	55	°	refs to y-axis
<b>Constant values</b>			
Spec. Heat capacity cp	4,18	kJ/kgK	
Spec. Heat capacity cv	4,13	kJ/kgK	
Viscosity water μ	0,0008	Pa s	
Density water ρ	1000	kg/m <sup>3</sup>	
Roller material λ	200	W/mK	
Spec. Heat capacity D-GTR	1,82	kJ/kg*K	
Thermal diffusivity D-GTR	1,4E-07	m <sup>2</sup> /s	
Thermal conductivity D-GTR	0,28028	W/m*K	
Roller pair torque	62	Nm	per roller pair
Speed ratio between rollers	1:1.1		
<b>Losses transmission</b>			
Straight, conical gears	86%		Gearbox, 3 stages
Chain rollers	98%		
Drive chain	98%		
Friction losses	98%		Bearings
Gears middle roller	98%		

#### 4.2.1 Parametric calculation 100 kg/hr D-GTR

Table 9 is an overview of the calculation input values. They correspond to the machine requirements, as determined at the beginning of the project.

The input values of the design are determined using an iterative method. The first design choices regarding the roller dimensions from paragraph 4.1.7 are used in these calculations. Other parameters like sheet thickness and the cooling water velocity were determined by changing the values in the model at a realistic way until reasonable output values were reached.

The constant values and transmission losses are values from the preliminary research and sources like textbooks. These values are fixed, and won't be changed during the design process.

Table 10 is an overview of the thermodynamical output values.

Table 10, Output parameters 100 kg/hr

<b>Main output values</b>					
<u>Property</u>	<u>value</u>	<u>unit</u>	<u>Property</u>	<u>value</u>	<u>unit</u>
<b>Cooling surface</b>			<b>Thermodynamical</b>		
Sheet width bottom	188,63	mm	Required heat flux	8230,4	W
1st nip	0,00707	m <sup>2</sup>	Temperature cw out	42,7	°C
middle	0,02531	m <sup>2</sup>	Mean temperature diff.	118,8	°C
2nd nip	0,00650	m <sup>2</sup>	Volume flow cw	0,000157	m <sup>3</sup> /s
bottom	0,11111	m <sup>2</sup>	Heat exch. Coef. 1st nip	83,2	W/m <sup>2</sup> K
<b>Effective sheet thickness</b>			Heat exch. Coef. Middle roller	218,5	W/m <sup>2</sup> K
1st nip	3,34	mm	Heat exch. Coef. 2nd nip	807,5	W/m <sup>2</sup> K
middle	2,6	mm	Heat exch. Coef. Bottom roller	532,6	W/m <sup>2</sup> K
2nd nip	0,32	mm	Heat flux 1st nip	69,9	W
bottom	0,5	mm	Heat flux middle roller	657,0	W
			Heat flux 2nd nip	623,4	W
			Heat flux bottom roller	7030,7	W
			total available heat flux	8381,0	W

The required heat flux output is 8230 W (Table 10). Using the parameters from Table 9, an available heat flux of 8381 W can be reached. It seems that the largest fraction of heat is dispersed on the bottom roller, where the sheet is relatively thin (0.9 mm) and a large contact area is reached. 7030 W is cooled via the bottom roller. The smallest nip height is 0.5 mm in the second stage, with an input height of 2.6 mm. Further testing will have to determine the calendering properties with these smaller nip heights.

The mechanical calendering properties are summarized in Table 13. These indicate the required rotational speed of the rollers and corresponding loads. The loads were used for dimensioning of the machine parts.

The remaining calculations including the thermal balance of the 100 kg/hr D-GTR case is described in appendix 3.

### 4.3 ROLLER DESIGN (COOLING SYSTEM)

The rollers are designed using the cooling design specifications of Table 9 and Table 10. The cooling water channels are designed to be as close as possible to the surface of the roller to optimize heat exchange. A cross-section of the rollers is illustrated in Figure 19.

#### 4.3.1 General design

The roller sleeve (outer drum) is comprised of 2 separate parts. The inner sleeve is made of steel (s235JR). The cooling water channel is designed to spiral along the roller surface. The spiral will be made in the inner sleeve using a lathe. The channel is shaped as an arc, ideal to support the roller pressure. The spiral radius is 5 mm. larger radiuses are expected to cause difficulties during fabrication.

The outer sleeve will be the outer shell of the roller. This part will be in contact with the rubber, and separates the rubber from the cooling water. It will be made from aluminium 6060 T6. The sleeve surface will get a hard- anodizing treatment. Anodizing creates an aluminium oxide layer, which prevents corrosion and has a hardness comparable to cutting tools. This layer is porous, and will be treated with PTFE to create an anti-stick layer. The 2 sleeves will be press- fitted into each other to create a strong sleeve to support the pressure.

The side walls of the rollers function as a support of the sleeves. They contain bores for the distribution of cooling water and have a cavity for the installation of clamp bushing to clamp the drum on the roller shaft.

The spacer ring and support are used to distribute radial forces to the shaft and prevent axial movement between the bearings.

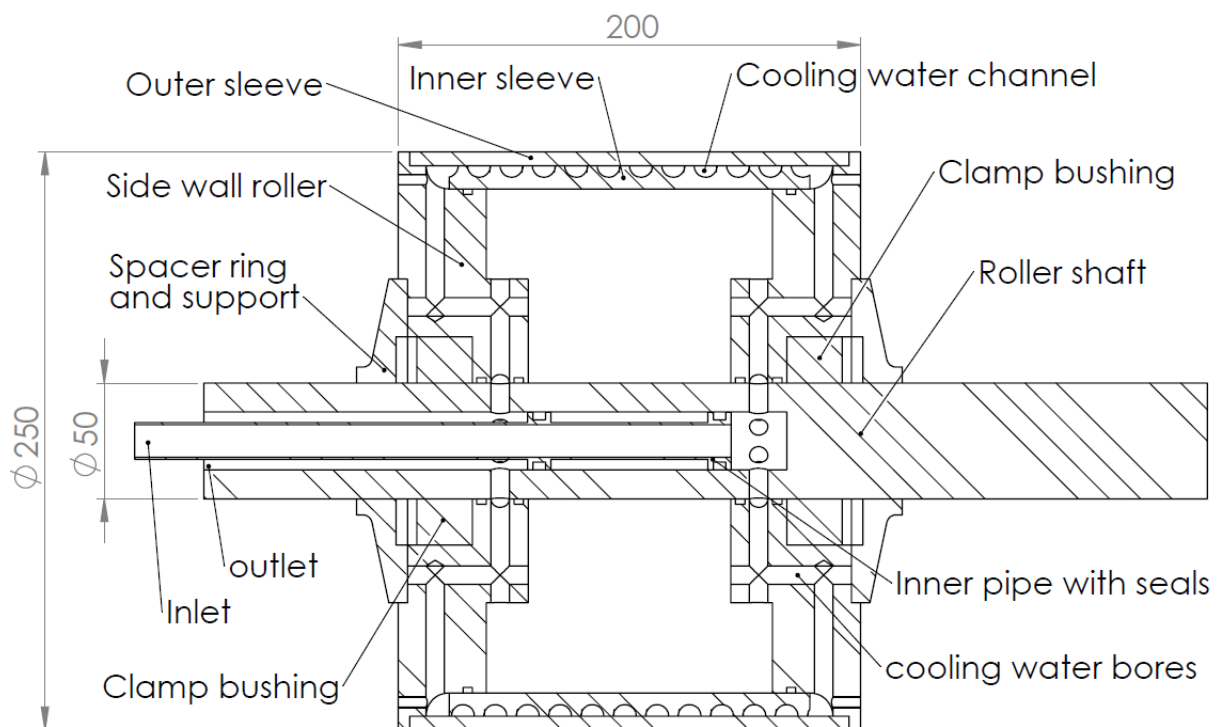


Figure 19, Roller cross section

The roller shaft is partially hollow, to allow water to flow through the rollers. An inner pipe is used to separate the inlet and outlet side of the water flow to allow the entire flow to pass through the cooling spiral.

The temperature difference between the inlet and outlet of the cooling water spiral inside the roller is designed to be as low as possible. The earlier mentioned flow of 0.157 kg/s value originates from a rated maximum cooling water velocity inside the spiral, which is determined to be 4 m/s. A higher water velocity creates a more turbulent water flow inside the spiral. This causes a resistance and drop in pressure. The cooling water system of the Polymer Science Park has a cooling water system, rated on a maximum pressure of  $5.8 \times 10^5$  Pa (580 kPa) and a volume flow of 3.88 dm<sup>3</sup>/s. The rated flow is through the roller is

$$\dot{V}_{cw} = \frac{\dot{m}_{cw}}{\rho} = \frac{0,157 \times 10^3}{1000} = 0,157 \left[ \frac{dm^3}{s} \right]$$

The flow through 3 rollers is 0,471 dm<sup>3</sup>/s which is well within limits. The pressure drop has to stay within limits as well. Computational fluid dynamics simulations were used to determine the pressure drop inside the rollers.

**4.3.2 Pressure drop rollers**

The flow through the roller spiral is rated 4 m/s. Higher flow velocities are expected to increase the pressure drop inside the rollers too much. Flow simulations were carried out to verify if this was the case. The necessary input for the simulations was

- A simplified 3D model for the roller with internal cooling
- Mass flow

The mass flow through the roller is determined by calculating the surface area multiplied by the velocity.

$$\dot{m}_{cw} = \dot{V}_{cw} \rho = v A \rho \quad (Eq. 22)$$

$$\dot{m}_{cw} = v \left( \frac{\pi d^2}{4} \right) \rho = 4 \times \left( \frac{\pi}{4} \frac{0.01^2}{2} \right) \times 1000 = 0,157 \frac{kg}{s}$$

As an input, the pressure at the outlet of the roller is at atmospheric pressure of 100 kPa. The result of the simulation is illustrated in Figure 20.

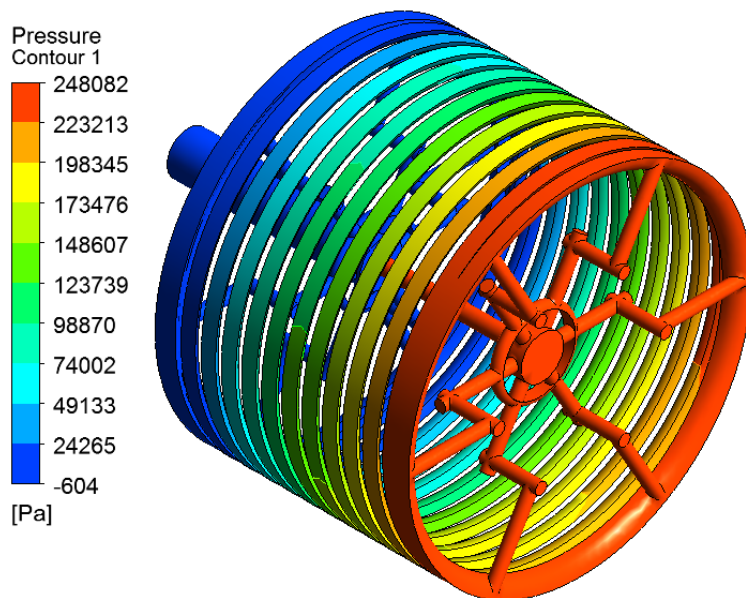


Figure 20, cooling water pressure in the cooling water channel

The pressure at the outlet is 0 Pa. This corresponds to the atmospheric pressure. The highest pressure is at the inlet, as expected. The pressure drop is 248082 Pa, which is approximately 250 kPa. This is well within the 580 kPa limit of the cooling system in the PSP.

The pressure drop is caused by the turbulent flow inside the cooling spiral. This is indicated by the colour difference, from blue to red, inside the spiral. The colours correspond to the amount of pressure.

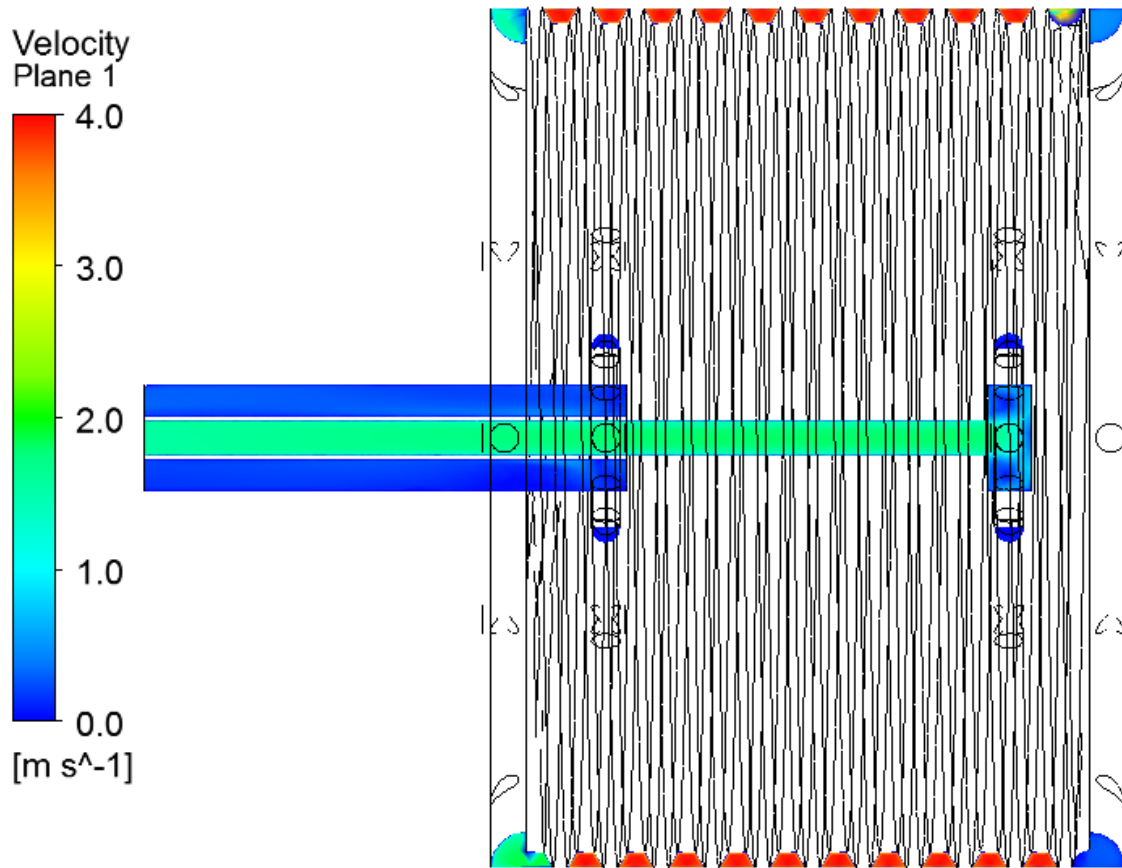


Figure 21, velocities inside the roller, cross section.

Figure 21 indicates the velocity profiles inside the roller. The maximum velocity is 4 m/s, as expected by the calculations.

The velocity at the inlet, outlet and bores need to be much lower for two reasons. First to prevent pressure drops, and second to reduce heat transfer between the inlet and outlet inside the shaft. A less turbulent flow reduces the convection value.

#### 4.4 RESULTS AND DISCUSSION

A parametric model has been made to determine the calendering specifications at different flow rates, temperatures and machine settings. The calculations in paragraph 4.2 represents one specific situation. It proves that it is possible to cool a mass flow of 100 kg/hr of D-GTR from 250 to 90°C, when the input values of Table 9 are used.

The rubber sheet is cooled one a single side. On the roller and cooled between 2 roller surfaces between the rollers. Heat transfer between the rollers has the same effect as cooling half the rubber sheet thickness, thereby almost doubling the heat transfer coefficient ( $K$ ). Switching the sheet to another roller also has another positive effect on the heat transfer; it raises the temperature difference. These positive effects in not included in the model, but will function as a safety factor during the development first design.

The thermodynamical calculations will be tested and evaluated during the test phase of this project. The testing phase won't be described in this report. The spreading properties of D-GTR will have to be tested as well.

Table 11 gives an overview of the calender specifications. The values originate from the calculations and the initial design choices.

*Table 11, design specifications cooling*

<b>Cooling design specifications</b>	<b>value</b>	<b>unit</b>
<b><u>General</u></b>		
Rated cooling capacity calender	8.4	kW
Rated rubber flow	100	kg/hr
Rated inlet temperature rubber (max)	250	°C
Rated outlet temperature rubber	90	°C
Rated cooling water flow	0,157	kg/s
Max outlet temperature cooling water	50	°C
Effective surface area roller	0,19	m <sup>2</sup>
<b><u>Rollers</u></b>		
Roller diameter	250	mm
Roller surface width	200	mm
Number of rollers	3	
Roller configuration	inclined 3 roller	

## 5 MECHANICAL DEVELOPMENT

The mechanical development of the machine is based on the parameters from the cooling development. The most significant loads of the machine are the necessary drive torque and the forces caused by the pressure between the rollers while calendering.

The torque is rated 520 Nm. The roller pressures depend on the machine setting. The parameters from the 100 kg/hr calculations (Table 9) are used for the roller forces calculations, because it's considered the highest load case. The activities to develop the mechanical part of the machine is the following.

- Determination of the roller pressures, forces and torque
- Making a global 3D model
- Modelling the transmission part of the machine
- Calculations of the bearing forces
- Calculations of the nip adjuster forces
- Detailed development (Strength calculations, simulations) of all parts, using the calculated forces as an input

The development of the calender parts will be done using development guidelines from the book 'machine parts' [14]. Mechanical simulations are also used, to determine mechanical stresses in frame parts, rollers and shafts.

### 5.1 CALCULATIONS AND GENERAL DESIGN

#### 5.1.1 Roller forces

The average roller pressure of 7.33 MPa is used to calculate the roller forces. The pressure is distributed on the roller surface, depending on the sheet width and length.

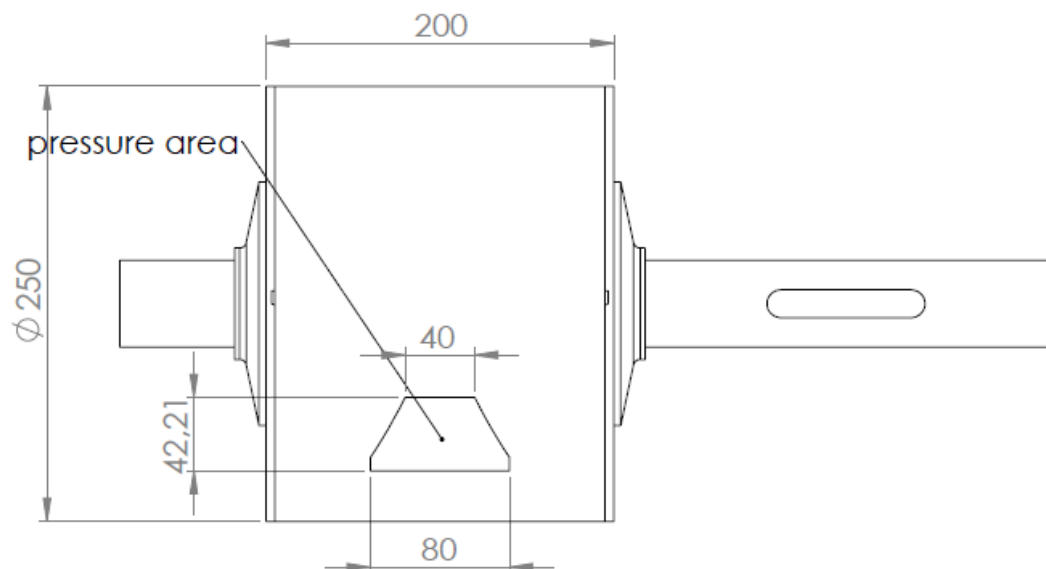


Figure 22, pressure area 1<sup>st</sup> nip. (Dimensions in mm)

The middle roller is illustrated in Figure 22. The pressure area are highlighted and correspond to the expected sheet widths. This is a top view of the roller. The upper roller has an inclination of 55 degrees, this is the reason why the pressure area is off centered. The pressure area may vary according to the nip heights and sheet width.

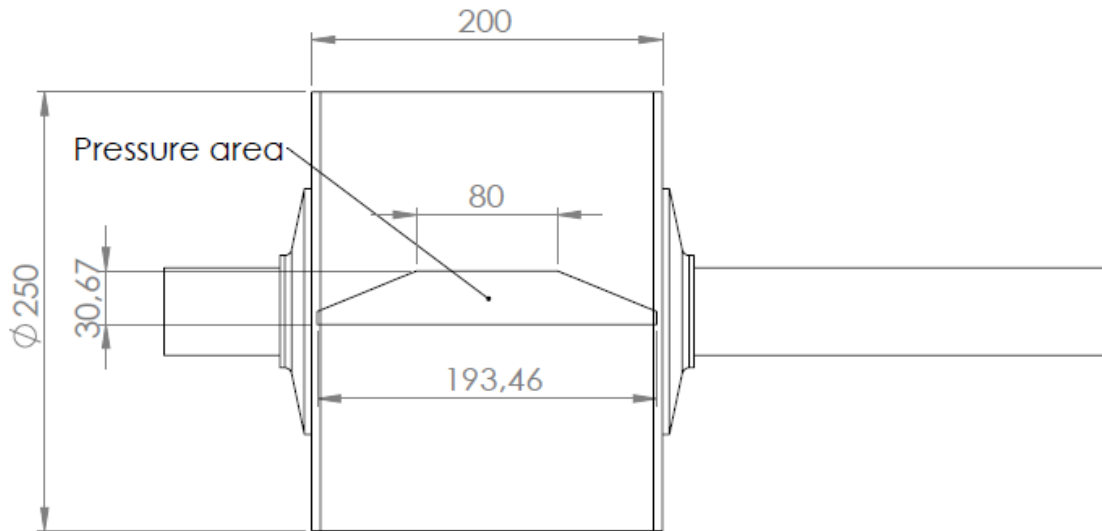


Figure 23, pressure area 2<sup>nd</sup> nip.

Figure 23 is bottom view of the pressure area on the middle roller, at the 2<sup>nd</sup> nip. The sheet thickness at the second nip is considerably lower as the thicknesses at the first nip. A relatively wide and short patch is the result. The total surface area used in further calculations is:

- 1<sup>st</sup> nip            3155.8 mm<sup>2</sup>
- 2<sup>nd</sup> nip            3170.2 mm<sup>2</sup>

The forces are calculated using the following equation,

$$p = \frac{F}{A_{1st}} \rightarrow F_{1st} = p \times A_{1st} = 7,33 \times 3155.8 = 23132 \text{ N}$$

$$p = \frac{F}{A_{2nd}} \rightarrow F_{2nd} = p \times A_{2nd} = 7,33 \times 3170.2 = 23237 \text{ N}$$

These resulting forces, along with the torque values are used to dimension the roller shaft, transmission parts, bearings, frame and nip adjusters.

The roller configuration is as an inclined 3 roller calender, as mentioned in chapter 4.1.7. The middle roller will be in a fixed position. The upper and bottom rollers should be able to move normal to the middle roller, to allow the nip height to be adjustable.

Figure 25 indicates the orientation of the roller forces cause by the roller pressure. The forces of the upper and bottom roller act normal to the nips.

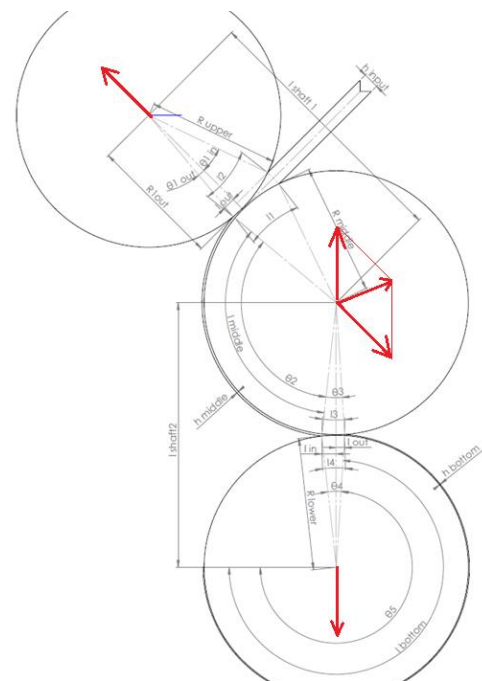


Figure 24, roller configuration with load vectors

### 5.1.2 Transmission

The next design step is to develop the transmission of the rollers. The rollers are supported on 2 sides by bearings. The roller shafts extend on two sides. One side of the shaft is where the transmission is constructed. Cooling water connections will be made on the opposite side of the shaft. A bore will be made on the cooling water side. The shaft on the transmission side will be solid, to ensure torsional stiffness and strength. The final transmission configuration is presented in Figure 25.

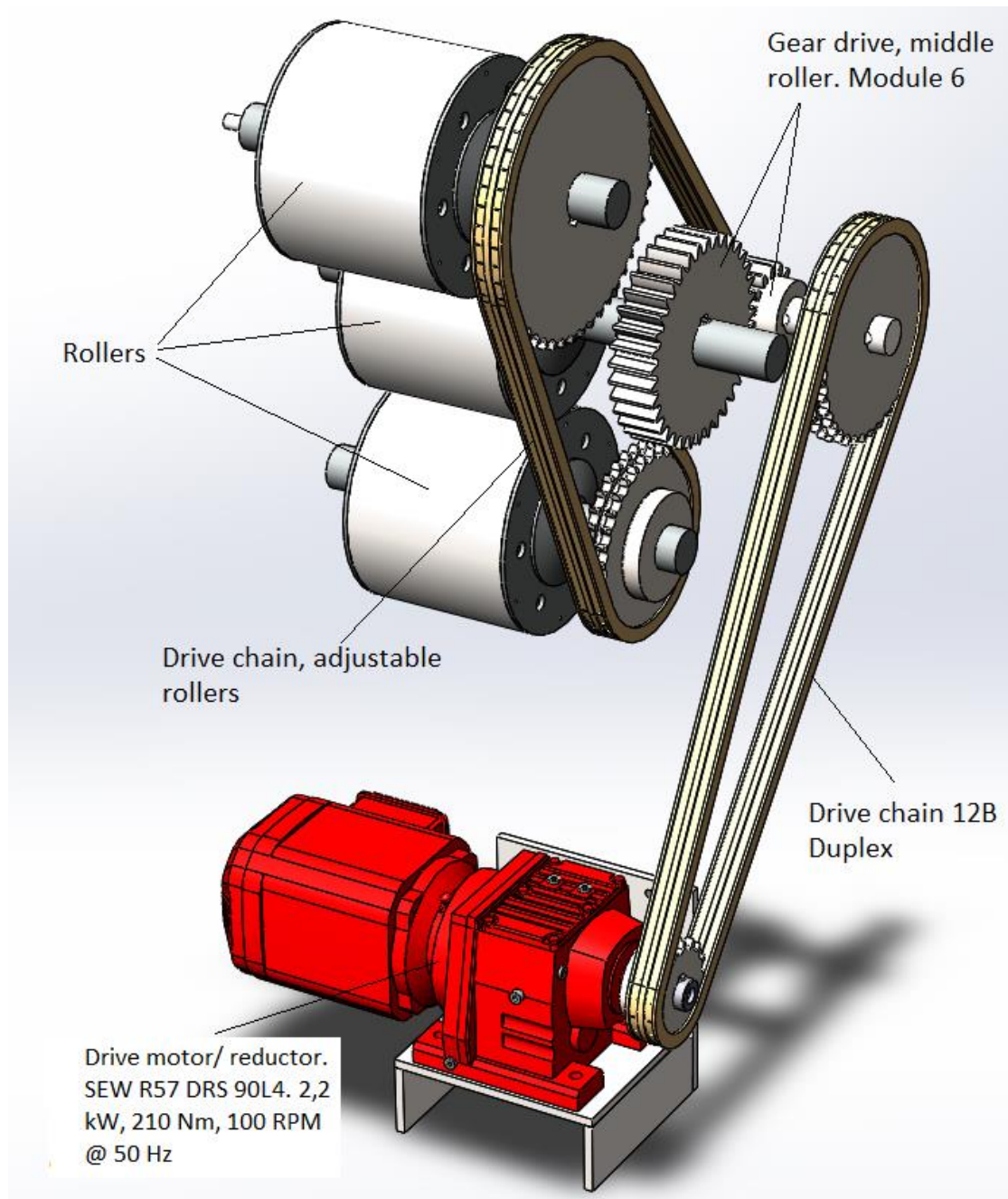


Figure 25, Transmission configuration.

Multiple reduction stages are implemented into the design to allow higher rotational speeds of the motor/ reductor. An extra shaft is installed to allow these multiple reduction stages. These

reduction stages, allows the motor/reductor to rotate at higher speeds, and lower torque values. As a result, a lighter gearbox is required between the machine and motor. This reduces the total costs of the motor.

The required motor/ reductor specifications are shown in Table 12. They are output values of the parametric calculations, for the 100 kg/hr case. The values are used to choose a suitable motor. A drive motor is selected using catalogues from the company SEW- Eurodrive.

Table 12, required motor/ reductor specifications

Motor/ reductor			
Drive power motor req.	145,9	W	
Rated drive power motor	281,7	W	@ 50 hz
Torque gearbox req.	29,20	Nm	
Speed ratio req. Gearbox	15,47	:	1

The motor will be controlled using a frequency drive. This is used to control the rotational speed of the rollers. The frequency of the Dutch power grid is 50 Hz. Frequency drives can be regulated from 0- 50 Hz. The required drive power was calculated to be 146 W. This value will correspond to a frequency of 30 Hz. This allows the rotational speed to be regulated to both higher and slower speeds. This makes the rated (required) drive power at 50 Hz is approximately 282 W. The chosen motor/ reductor is shown in Figure 25, it is expected to be overpowered this is caused by early assumptions during the design phase, though this should not affect the performance of the calender.

The middle roller has a fixed position in the frame, the shaft distance between the extra shaft and middle roller shaft is fixed, making it ideal for a gearwheel drive. The upper and bottom rollers should be able to move normal to the middle roller, to allow nip adjustability. This makes a gear drive not ideal. Other options are either a belt drive or chain drive. A comparison was made using the using the parameters

The decision is made to use a chain drive to drive the upper and lower rollers. The main reason was the price differences between the two options. A belt drive type Optibelt Omega 8M (Figure 27) was calculated to be usable to drive the rollers. The downside of a belt drive:

- Necessary belt width 85mm
- High costs
  - o Belt €1305, -
  - o Pulleys €782, -
- Belts can't be shortened/ lengthened.

The chain drive is considerably cheaper. A standard 12B-2 (duplex) chain along with the necessary chain wheels costs.

- Chain 12B-2 (5 meter) €144, -
- Chain wheels (including drive chain between the machine and reductor) €369, -

The required rotational speeds of the transmission depend of the D-GTR flow and nip settings. Rotational speed calculations are implemented into the parametric model. The transmission calculation output, for the 100 kg/hr case are summarized in Table 13.



Figure 26, Optibelt Omega

Table 13, Transmission output

Transmission			
RPM middle roller	11,2	RPM	
RPM bottom roller	12,3	RPM	
RPM upper roller	10,1	RPM	
Between shaft RPM	26,8	RPM	
Reductor output RPM	59,9	RPM	@ 30 hz
Rated RPM reductor	99,8	RPM	@ 50 hz
Drive power motor req.	1316,4	W	
Rated power motor	2334,1	W	@ 50 hz
Torque gearbox req.	223,29	Nm	
Speed ratio req. Gearbox	14,03	: 1	

### 5.1.3 Bearings and nip adjuster loads

The transmission forces, in addition to the roller pressure forces are the basic loads acting on the machine. The upper and bottom rollers are supported by two bearings. The drive gears are designed to be free floating as shown in Figure 28. This allows the sprockets to be changeable, when different speed ratios are required. And allows the nip height to be adjustable.

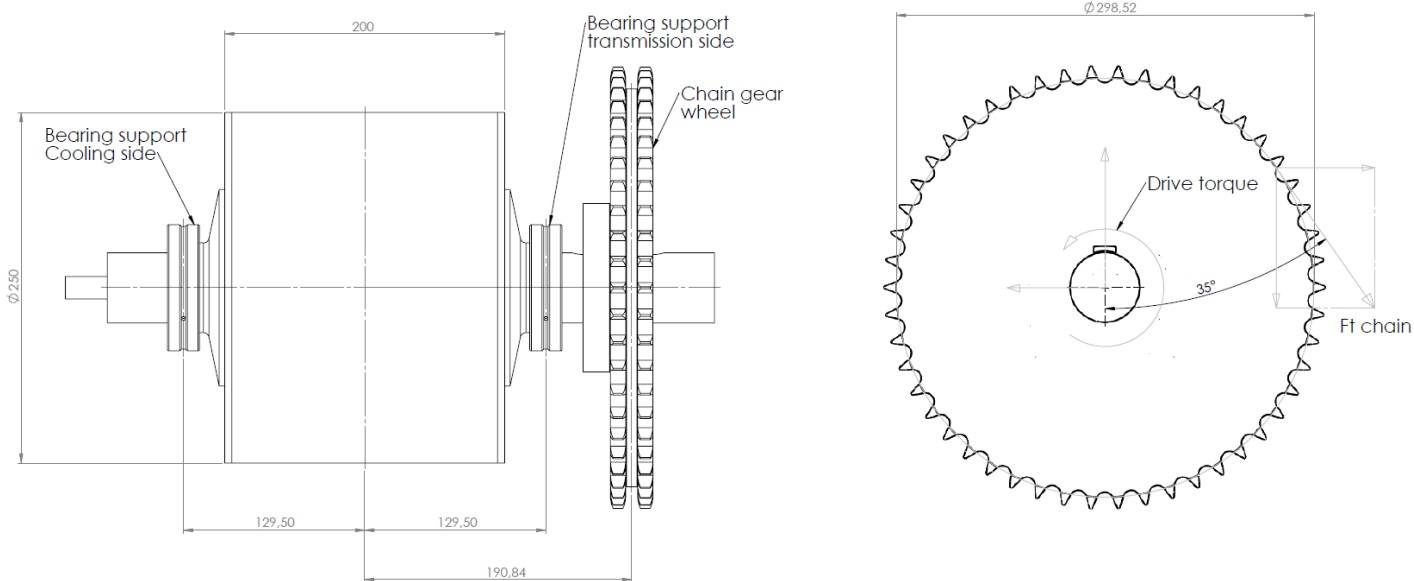


Figure 27, Upper Roller, including bearings and drive

The free floating sprocket causes additional bending, torsional and shear forces, which are supported by the bearing on the transmission side. The fixed position of the middle roller makes it possible to install an additional bearing to support the drive gear. The effects of an additional bearing are

- Reducing deformation of the roller shaft
- Lowering the maximum reaction forces
- Reducing the necessary shaft diameter

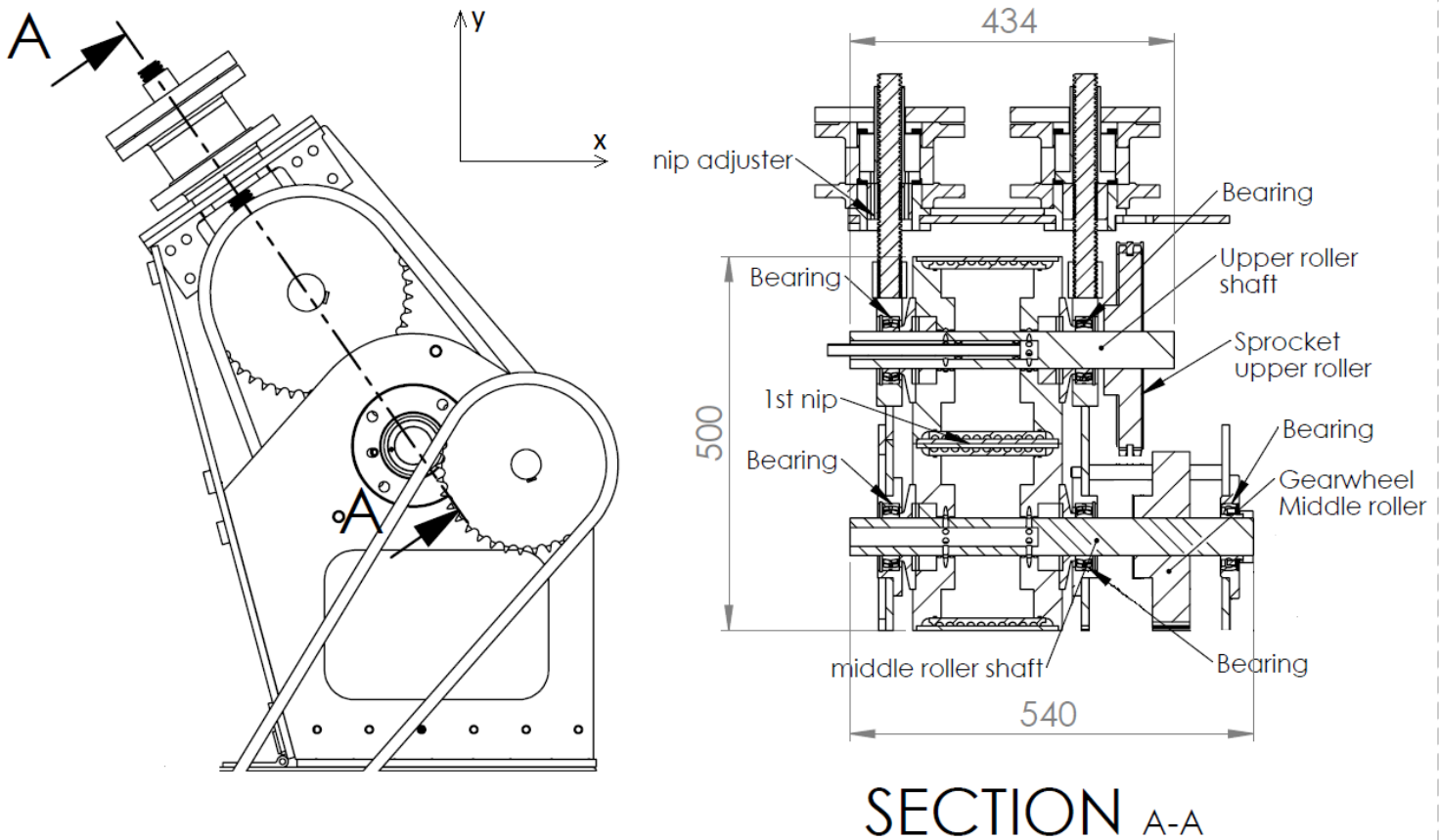


Figure 28, Cross section upper and middle rollers

A cross-section of the upper part of the machine is illustrated in Figure 29, it shows the difference between the upper and middle roller drive, and the additional bearing near the gearwheel. The x and y-axis are indicated too. The directions of x and y in this figure corresponds to all calculations in this chapter.

The reaction forces are calculated using manual calculation and verified using Solidworks simulations. The calculations are implemented into the parametric model to allow further usage of the calculation outputs. The calculated reaction forces will be used to design bearing housings, the frame and nip adjusters, combined with a spring loaded safety. The input values for the simulations are the roller pressure forces are

- Roller pressure forces (chapter 5.1.1)
  - o 23132 N 1<sup>st</sup> nip
  - o 23237 N 2<sup>nd</sup> nip
- Drive forces
- Estimated mass of the roller, shaft and drive gear/sprocket
  - o Roller, 42 kg
  - o Gear/ sprocket, 5 kg
- Roller shaft dimensions (distances between the bearings, sprockets and forces)

The upper roller drive forces are determined using the geometry of the transmission, torque and roller rotational speed. The upper and bottom roller are driven using a chain drive, as shown in Figure 28.  $F_{t\ chain}$  is the static pulling force to rotate the roller, which is the necessary force to start moving the roller. The dynamic forces used to get the roller in motion is marginal compared to the static pulling force. The static pulling force is determined by the following equation

$$F_{t\ chain} = \frac{T}{d_{sprocket} \times \pi \times n_{roller}} \quad (Eq. 22)$$

In the case of the upper roller it's

$$F_{t\ chain} = \frac{520}{0.273 \times \pi \times \left(\frac{10.12}{60}\right)} = 3456,4\ N$$

The drive forces, roller pressure forces and reaction forces act in certain directions. The drive force for example, has an angle of 35° relative to the y-axis (vertical axis). The x and y components of the drive force can be calculated using this angle. Shaft calculations are calculated along the x-axis and y-axis. The resulting forces are calculated using Pythagoras ( $a^2 + b^2 = c^2$ ).

The simulation of the upper roller shaft is presented in Figure 29. The upper roller had 4 joint where either fixtures or external loads are applied. The indicated values in the illustration represent the reaction forces of the bearings.

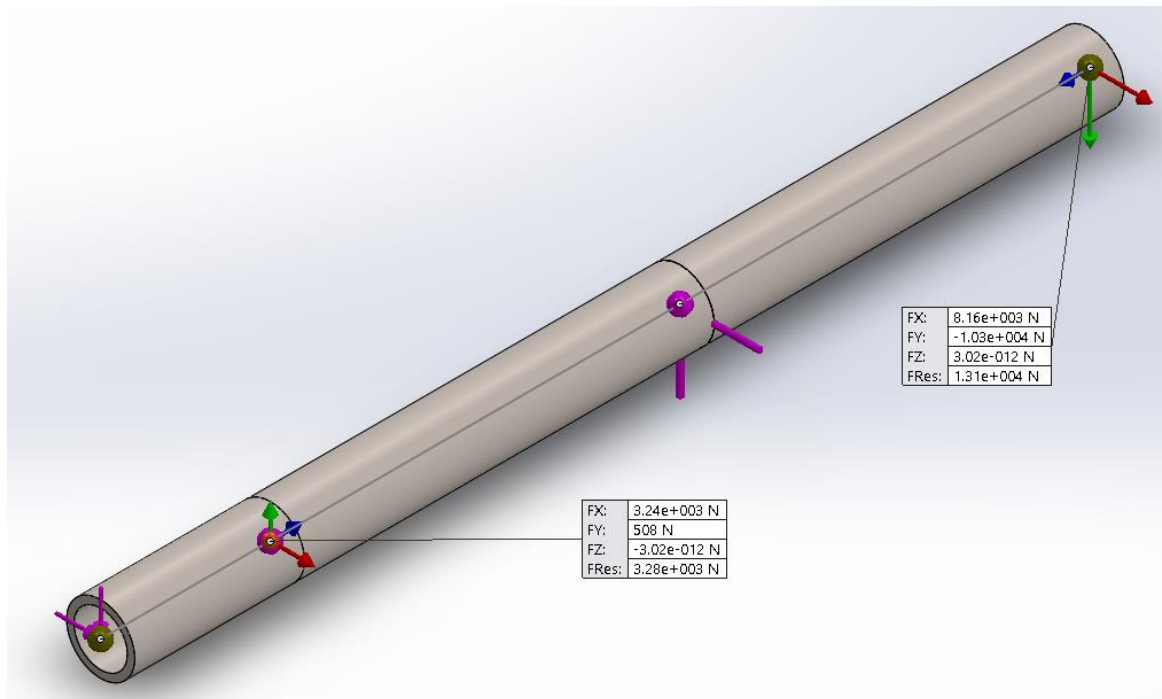


Figure 29, Bearing reaction forces upper roller

The middle roller has an extra joint, representing the third bearing. This is illustrated in Figure 30, along with the reaction forces acting on the bearings.

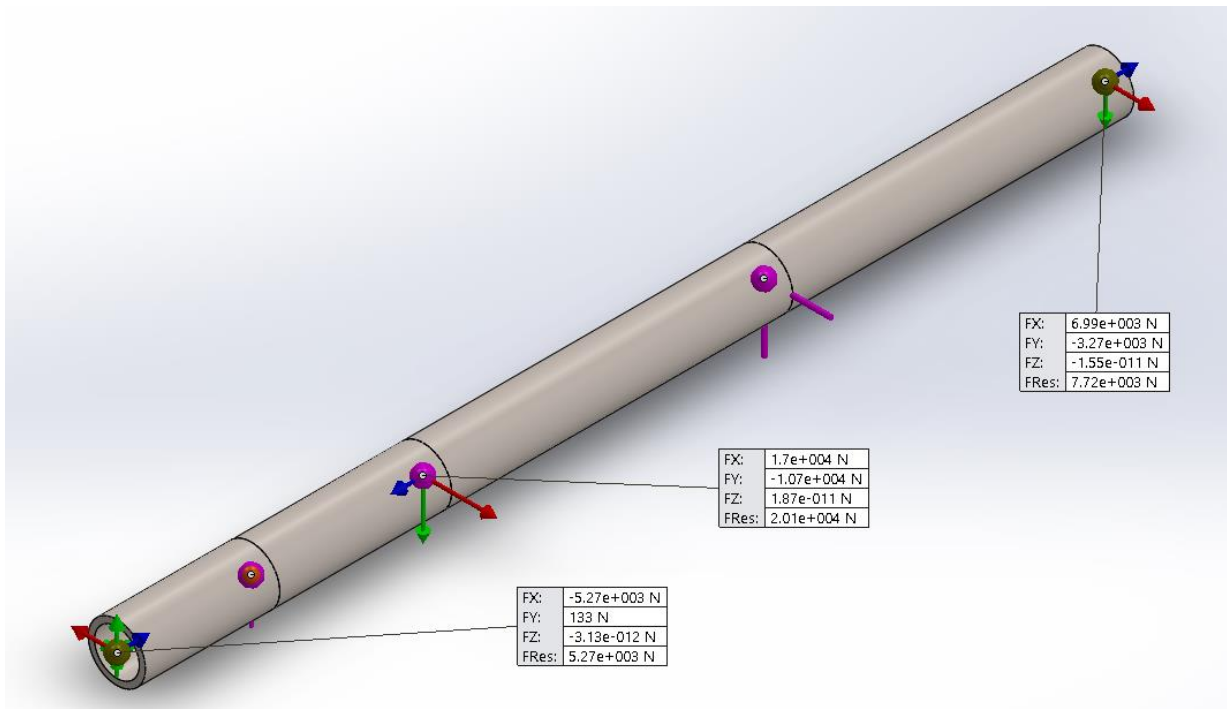


Figure 30, bearing reaction forces middle roller

The bearing forces, in the 100 kg/hr D-GTR case are summarised in Table 14. The x-axis is normal to the front of the machine and the y-axis is normal to the top plane of the machine. The use of straight teeth gears and chains prevent any axial forces along the shaft.

Table 14, bearing forces

Reaction forces				
<u>Output, middle roller</u>	x	y	res	Angle rel. to x
FB1	6990,00	-3270	<b>7717,1</b> N	-25,07 °
FB2	17000,00	-10700	<b>20087,1</b> N	-32,19 °
FB3	-5270,00	133	<b>5271,7</b> N	-1,45 °
<u>Output, upper roller</u>	x	y	res	Angle rel. to x
FB1	8164,2	10297,4	<b>13141,2</b> N	51,59 °
FB2	3244,72	566,82	<b>3293,9</b> N	9,91 °
<u>Output, bottom roller</u>	x	y	res	Angle rel. to x
FB1	444,8	13445,9	<b>13453,3</b> N	88,11 °
FB2	4500,60	2372,08	<b>5087,5</b> N	27,79 °

These values will be used to determine the size and specifications of the bearings, roller shaft and the nip adjusters. The shaft diameter calculations also require the moments acting on the rollers. These are plotted using Solidworks.

The remaining roller parts like the side walls, roller surface sleeve and spacers are simulated using static simulations, using the know external forces as an input to determine the stresses in the parts.

### 5.1.4 Bearing choices

The rollers, transmission shafts and nip adjusters contain bearing. The determination and calculations for the bearings are derived from Rollof/Matec [14]. The necessary values to determine the suitable bearings on the different parts are

- Bearing forces ( $F_{res}$ )	Table 14
- Rotational speed of the bearing ( $n$ )	Table 13
- Specified amount of operating hours ( $f_L$ )	200 hours
- Running conditions factor ( $f_s$ )	2 (heavy load)

The rotational speed of the roller shafts is 10.1-12.3 RPM (when calendering 100 kg/hr). Each type of bearing has a certain load rating, which is either the allowable force in the radial or axial direction. There are two types of load ratings. The basic dynamic load rating ( $C$ ) and the basic static load rating ( $C_0$ )

#### Static loads (roller bearings)

The static load rating is the defining rating with rotational speeds  $<10$  RPM [14]. The roller bearing are determined using this. The requires static load rating is determined by the following equation

$$C_0 = P_0 \times f_s \quad (Eq. 23)$$

$P_0$  is the resulting bearing load, corresponding to  $F_{res}$  in Table 14. This is valid for exclusively radial loads.  $f_s$  is a static load factor, depending of the amount of shocks, jolts and vibrations the bearing will endure. The criteria are

- Easy vibration less running	$f_s = 0.5 - 1.0$
- Normal running, light shocks and vibrations	$f_s = 1.0 - 1.5$
- Heavy shocks, jolts and vibrations, and axial bearings	$f_s = 1.5 - 2.5$

Calendering is considered a heavy process. An  $f_s$  value of 2 will be used to determine the bearings. Self-aligning bearing will be used to support the roller shafts. This allows any deformation of the roller shaft to be compensated, hereby preventing unexpected bending forces to be strain the bearings, preventing damage to the bearings.

Two types of self-aligning bearings will be used in the design. Spherical roller bearings, and insert ball bearing, combined with their corresponding bearing housings as illustrated in Figure 32. Using equation 23 and the resulting reaction forces in Table 14, the required static load ratings of the bearings are

Table 15, required static load ratings

Upper roller	$F_{res}$ [N]	$f_s$	$C_0$ req. [N]
FB1	13141,2	2	26282
FB2	3293,9	2	6588
Middle roller			
FB1	7717,1	2	15434
FB2	20087,1	2	40174
FB3	5271,7	2	10543
Bottom roller			
FB1	13453,3	2	26907
Fb2	5087,5	2	10175

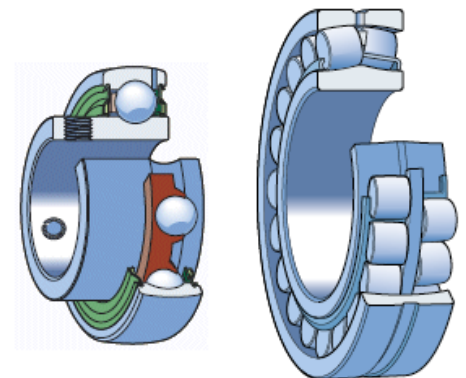


Figure 31, insert ball bearing (left), spherical roller bearing (right)

### Dynamic load (between shaft)

The remaining transmission parts will rotate at higher rotational speeds >10 RPM. The required dynamic load rating is determined using the following equation

$$C = P \times \frac{f_L}{f_N} \quad (\text{Eq. 24})$$

P is the dynamic radial load on the bearing in [N],  $f_L$  is a running hour factor, calculated by equation 25 and  $f_N$  is a rotational speed factor, determined using equation 26.

$$f_L = \sqrt[p]{\frac{L_{10H}}{500}} \quad (\text{Eq. 25})$$

$$f_N = \sqrt[p]{\frac{33\frac{1}{3}}{n}} \quad (\text{Eq. 26})$$

Both equations contain a lifecycle exponent (p). This exponent is 3 for ball bearings and 10/3 for roller bearings. The rotational speed (n) should be entered as [RPM] in this case.  $L_{10H}$  is the required running hours. The required running hours are 200. Using equation 25

The between shaft will be supported by standard ball bearings. The between shaft will endure the transmission loads only, without the roller forces. The maximum bearing load on the between shaft bearings was determined to be 5223 N, for the 100 kg/hr case.

In case of the between shaft, the running hour factor is

$$f_L = \sqrt[3]{\frac{200}{500}} = 0.74$$

The rotational speed of the between shaft is taken from Table 13, in which the rotational speed is 26.8 RPM. The rotational speed factor is

$$f_N = \sqrt[3]{\frac{33\frac{1}{3}}{26.8}} = 1.08$$

The required dynamic load rating for the between shaft bearings, using the determined force of 5223 N is

$$C = 5223 \times \frac{0.74}{1.08} = 3579 \text{ N}$$

See appendix 3, chapter 1 for the chosen bearings.

**5.1.5 Nip adjuster design and forces**

The bearings of the upper and bottom rollers are installed into linear movable bearing housings. The bearing housings will be installed in the linear guide ways, mounted to the frame. The bearing housings of the upper and lower rollers are able to slide normal to the middle roller. The nip adjusters of the cooling calender is designed to have multiple functions

- Adjusting the nip height of the rollers
- Supporting the roller pressure forces
- Function as an overpressure safety

The linear bearing housing of the upper roller is illustrated in Figure 32. The trapezium thread allows the roller adjustability and guides the roller forces to the nip adjuster. The bottom roller has a similar bearing block. The difference is that the bottom roller is fitted with standard ball bearings, because of expected lower loads.

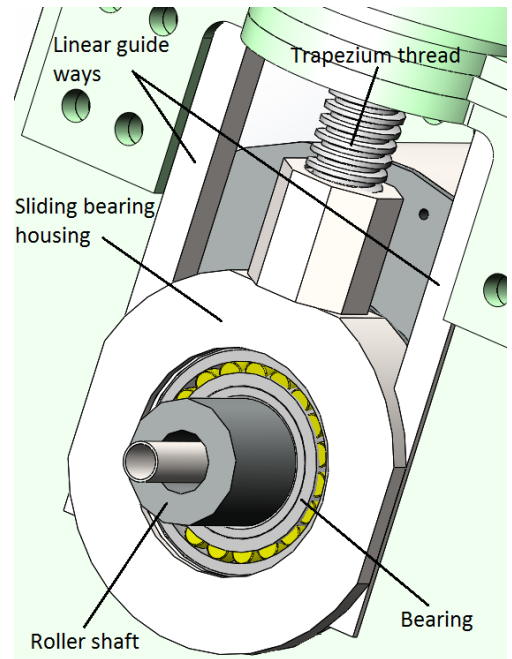


Figure 32, Sliding bearing assembly

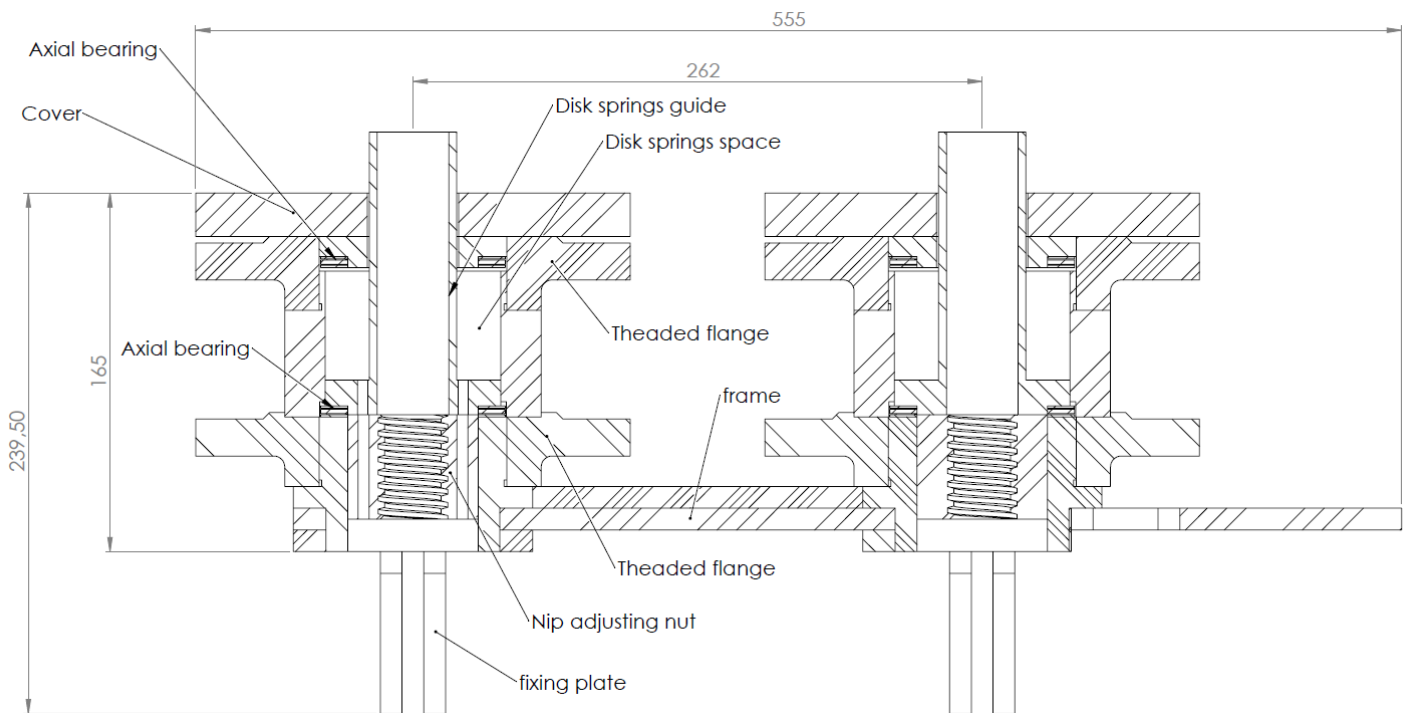


Figure 33, Upper roller nip adjuster assembly (cross- section)

The resulting reaction forces, with their corresponding angles from Table 14 have to be supported during operation. The radial forces are supported by the frame. The axial forces are guided through the trapezium spindle, via the nip adjuster nut and disk springs guide to the frame (as illustrated in Figure 34). A column of disk springs will be installed into the disk springs space to allow movement of the nip adjusting nut during overpressure. Axial needle bearings will be installed between the disk columns to allow the nut to turn when the disk springs are

under tension. The adjusting nut is designed to be turned for nip adjustment. The spindle will remain stationary.

Each bearing housing endures different forces. The maximum calculated forces for the 100 kg/hr case are used as design values. The forces in  $F_{B1}$  of the upper roller are shown in Figure 34.

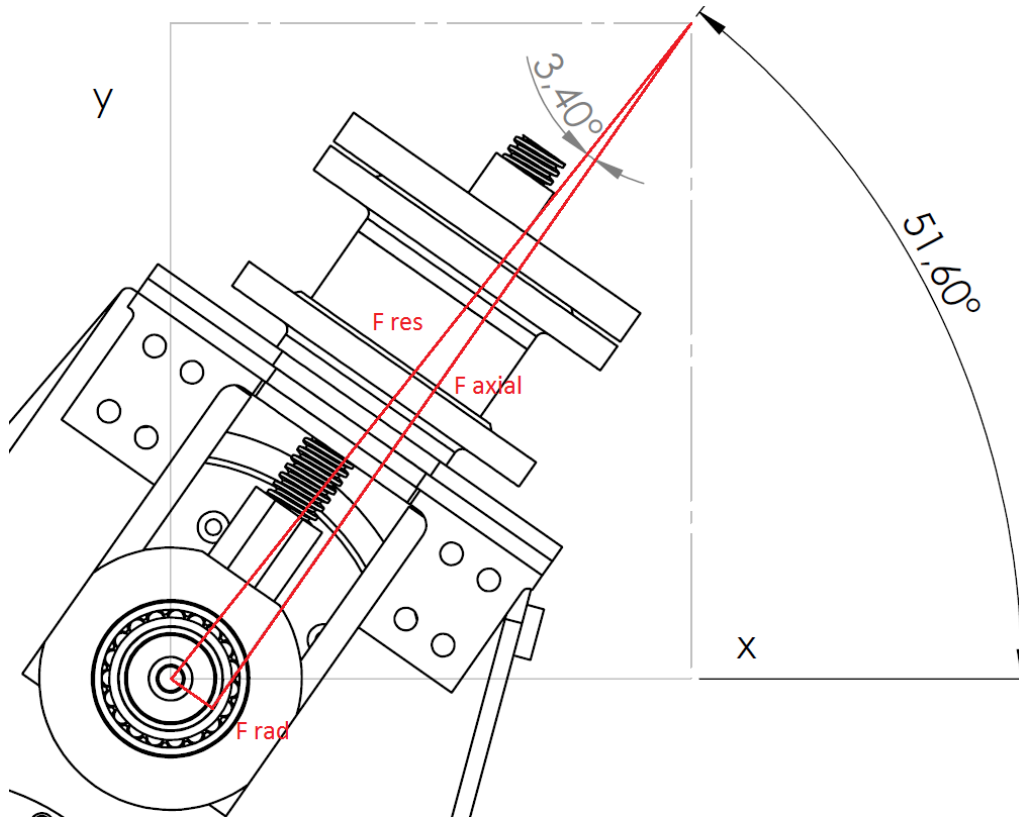


Figure 34, Forces on  $F_{B1}$  upper roller

$F_{res}$  is the resulting force from Table 14.  $F_{axial}$  is the pushing force through the trapezium spindle.  $F_{rad}$  is the radial bearing force, supported by the frame. The calculated resulting force angles are used to calculate the loads. These are summarized in Table 16.

Table 16, Roller, bearing forces

<b>Roller, bearing forces</b>				
<b>Output, upper roller</b>	$F_{res}$ [N]	angle [rad]	$F_{axial}$ [N]	$F_{radial}$ [N]
FB1	13141,2	0,90	13117,9	781,4
FB2	3293,9	-0,17	1396,8	2983,0
<b>Output, bottom roller</b>				
FB1	13453,3	-1,54	13445,9	444,8
FB2	5087,5	-0,49	2372,1	4500,6

$F_{axial}$  is used to determine:

- Trapezium thread diameter, pitch and necessary thread length
- Disk spring specifications
- Frame strength (Solidworks simulations)

5.1.6 Trapezium thread calculations

The main function of the trapezium treads is to adjust the roller nip height. A secondary function is to distribute the roller forces to the frame. The trapezium spindle is spring loaded to prevent overpressures which may damage the construction. This safety is the third function.

The strength of the spindles and nuts of the nip adjusters has to be sufficient to endure the axial bearing block forces from Table 16. There are 3 main fail criteria concerning the spindle and nuts

- Failure by compression stress
- Buckling of the spindle
- Thread damage

The maximum resistance to buckling and compression depends of the chosen spindle material and inner diameter ( $d_i$ ) of the spindle (d3 Figure 35). The maximal compression strength depends of the material. It is determined using the Rollof/Matec [14]. Standard trapezium thread (DIN 103/ NEN 2781) are used. Standard trapezium threads are available in multiple diameters. These diameters are normally linked to a certain pitch, according to the standard. The thread size is indicated by the following code.  $TR(outer\ diameter) \times (pitch)$

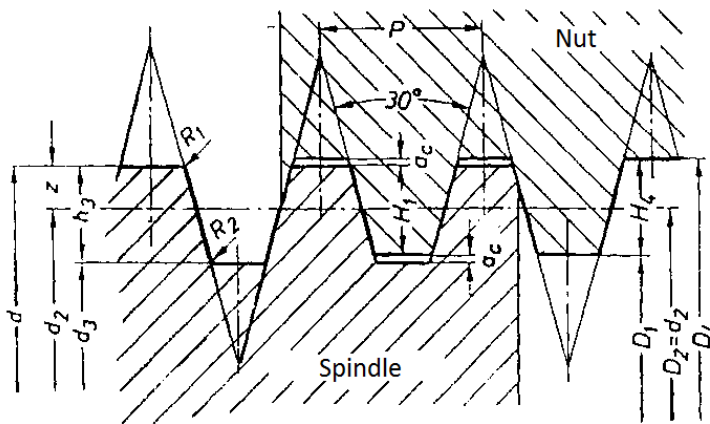


Figure 35, Trapezium thread

A generally used spindle material is C35. It has a permissible strength ( $\sigma_{tdwn}$ ) of 250 Mpa. This value is used to determine the maximum axial force, for a chosen trapezium thread. The equation used for the compressive strength

$$F_{axial} = \sigma_{tdwn} \times \frac{\pi}{4} d_i^2 \quad (Eq. 23)$$

Buckling is another way of the spindle to fail. The permissible buckling force depends on the slenderness of the column. This is the length of the spindle compared to the diameter. The spindles are fixed are installed in nuts, making it fixed joints. The equation to calculate the permissible axial force for buckling is

$$F_{axial} = \frac{\pi^2 EI}{(0.5L)^2} / s_f \quad (Eq. 24)$$

In which E is the elastic modulus [N/mm<sup>2</sup>], I is the moment of inertia [mm<sup>4</sup>] and L is the length between the fixtures [mm] and  $s_f$  is a safety factor. The constant values used during these calculations are

*Table 17, constant calculation values*

<b>E</b>	210000	Mpa
<b>L upper</b>	57	mm
<b>L bottom</b>	63	mm
<b>Sf</b>	3	

Both the maximum compression force and maximum buckling force has to be calculated for a certain chosen spindle size. The lowest permissible force from these calculations is considered critical.

Trapezium thread assumptions have been made early in the design, using the standard hole diameter of the linear roller bearing housings of the bottom roller. TR28x5 is used for the bottom roller adjusters. The upper roller adjuster has TR32x6 thread. The strength is checked using the 100 kg/hr mass flow values, and material properties of C35. The results for the upper roller

$$F_{axial} = 250 \times \frac{\pi}{4} 25^2 = 201062 \text{ N}$$

$$F_{axial} = \frac{\pi^2 210000 \times (\frac{\pi}{64} 25^4)}{(0.5 \times 57)^2} / 3 = 16309410 \text{ N}$$

The results for the bottom roller:

$$F_{axial} = 250 \times \frac{\pi}{4} 23^2 = 103868,9 \text{ N}$$

$$F_{axial} = \frac{\pi^2 210000 \times (\frac{\pi}{64} 23^4)}{(0.5 \times 63)^2} / 3 = 9564404 \text{ N}$$

These calculations conclude that the diameter of the threads are strong enough to handle the forces, considering the maximum axial force of 13446 N (Table 16).

Standard nut sizes are used for the nip adjusters. These have certain thread lengths, according the specifications of the supplier (Machinefabriek Harderwijk BV). Calculations of the thread surface pressure are made, to ensure thread strength. The calculation method is derives from Rollof/Matec [14]. The surface pressure equation is

$$p = \frac{F_{axial} \times P}{l_1 \times d_2 \times \pi \times H_1}$$

- $p$  is the surface pressure [N/mm<sup>2</sup>]
- $P$  is the pitch [mm]
- $l_1$  is the nut length [mm]
- $d_2$  is the pitch diameter [mm]
- $H_1$  is the flank overlap [mm]
- $\bar{p}$  is the admissible surface pressure.

The nut doesn't rotate during load condition, only when adjusting the nip height. Steel nuts are used in the machine, which are good to withstand static loads. The admissible surface pressure for steel on steel contacts is determined to be 10 Mpa [14].

The surface pressure results are given in Table 18, along with the standard nut dimensions. The calculated values are lower than the admissible pressure, meaning the thread is strong enough.

Table 18 nut dimensions

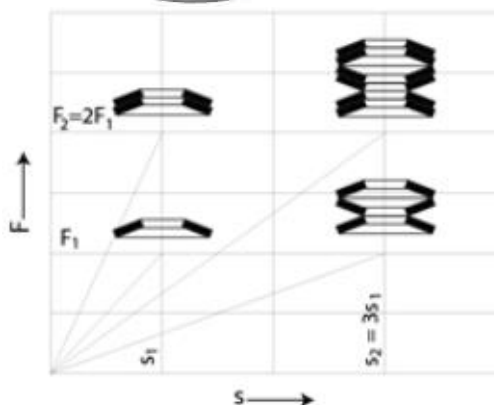
Nut sizes	nut length [mm]	nut outer diam. [mm]	admissible pressure [Mpa]	calculated pressure [Mpa]
TR28 x 5	42	60	10	4.66
TR32 x 6	48	60	10	6.15

### 5.1.7 Disk spring calculations

The disk springs are used to compensate for unexpected roller forces. This might be caused by scrapers or other solid object being pulled through the nip, while calendaring. The rollers are design00ed to be spring loaded. This makes the rollers able to move apart, hereby reducing the chance of further damages.



Disk springs are chosen, for their linear spring properties, and ability to handle high forces with small displacements. The disks can be stacked in different ways to adjust the spring characteristics, as illustrated in Figure 37. As illustrated in the graph, stacking them the same face up or upside down, either doubles the required force, or doubles the stroke.



This makes disk springs ideal for the calender, the springs may be adjusted according to the required load, depending on machine setting.

A pre-tension has to be applied on the disk stack to prevent the rollers from moving apart with lower loads. The pre-tension has to be a fraction bigger than the expected axial forces from Table 16. The pre-tension of the disk stack is achieved by compressing the disk stack inside the upper and lower frame.

Figure 36, disk spring stack, and stacking effects

The compression height are calculated using the required pre-tension and disk spring dimensions and characteristics. The required disk spring parameters, according to Figure 38 are

- Outer diameter ( $D_o$ )
- Inner diameter ( $D_i$ )
- Thickness ( $T$ )
- Spring height unloaded ( $L_0$ )
- Spring height max load ( $L_{0,75}$ )
- Spring force at max load ( $F_{0,75}$ )

These values are taken from data sheets of the supplier [15]. The inner and outer diameters of the springs depend on the design choices. The inner diameter for example depends of the diameter of the trapezium spindle.

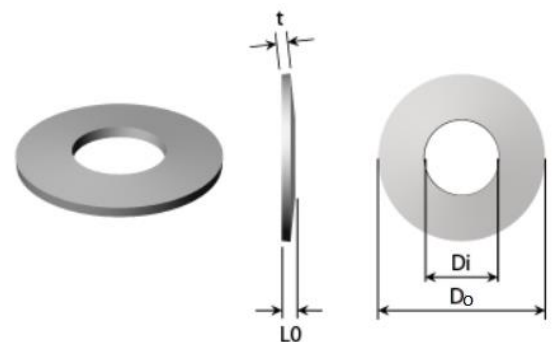


Figure 37, disk dimensions

The inner and outer diameter are constant values during calculations. The thickness of the disk may change according the requirements. The diameters of the upper roller disk stacks are:

- $D_o = 80$  mm
- $D_i = 41$  mm

The diameters of the bottom roller disk stacks are:

- $D_o = 63$  mm
- $D_i = 31$  mm

The pre-tension force is  $1,5 \times F_{axial}$ , which in the case of the 100 kg/hr mass flow is rated 20169 N. The frame is designed to withstand ever higher forces, up to 60000 N per nip adjuster. The rollers are designed to resist distributed roller forces up to 100000N.

Multiple disks can be stacked as in Figure 37 on the left. Disks stacked this way is called a pack. Disks on top of each other doubles the required force to reach a certain stroke. The amount of disks in a pack is called  $n_1$

Disk packs stacked the other way around (Figure 37 right) are called columns. This doubles the stroke when applying a certain force. The amount of columns in a stack is called  $n_2$ . The stack height ( $L_{0,stack}$ ) is calculated using the following equation

$$L_{0,stack} = L_0 + ((n_2 - 1) \times T) \times n_1 \quad (Eq. 26)$$

Disk springs tend to have linear characteristics until 75% of their maximum stroke, where the maximum stroke  $s_{max} = L_0 - T$ . This means the maximum rated stroke of a disk  $s_{0.75} = s_{max} \times 0.75$

Suppliers include the corresponding force to  $s_{0.75}$  in the data sheets. These values are necessary to calculate the pre-tension force when compressing a stack. The spring stack force, as a function of the percentage of compression is calculated using

$$F_{stack} = (F_{0.75}/0.75) \times s_{pre-load\%} \times n_1 \quad (Eq. 27)$$

The height of the stack, as a function of the percentage of compression is calculated using

$$L_{stack} = L_{0,stack} - \left(\frac{L_{0.75}}{0.75}\right) \times s_{pre-load\%} + (n_1 - 1) \times T \times n_2 \quad (Eq. 28)$$

## 5.2 RESULTS AND DISCUSSION

### 5.2.1 Specifications

The calculation output from chapter 5.1 are used during the design phase of the project. The loads are known and the first design choices have been made. The results function as a guide during the design process. The general machine specifications are summarized in Table 19.

*Table 19, Machine specifications*

<b>Machine specifications</b>	<b>value</b>	<b>unit</b>
<b><u>General</u></b>		
Rated cooling capacity calender	8,4	kW
Rated rubber flow	100	kg/hr
Rated inlet temperature rubber (max)	250	°C
Rated outlet temperature rubber	90	°C
Rated cooling water flow	0,157	kg/s
Max outlet temperature cooling water	70	°C
Total surface area rollers	0,471	m <sup>2</sup>
<b><u>Dimensions an weight</u></b>		
Height machine	1,62	m
Length machine	1,00	m
Width machine	0,94	m
Weight (approximation)	425	kg
<b><u>Rollers</u></b>		
Roller diameter	0,25	m
Roller surface width	0,2	m
Amount of rollers	3	
Roller configuration	inclined 3 roller	
incline angle	55	°
<b><u>Transmission</u></b>		
Power drive motor/reductor	2,2	kW
Max torque motor/reductor	263	Nm
RPM output reductor at 50 Hz	100	RPM
RPM middle roller	10,31	RPM
RPM upper roller	9,34	RPM
RPM bottom roller	11,36	RPM

Earlier design choices have been made in the course of this project, to ensure an early start of production of the less critical parts. Assumptions have been made concerning calendaring roller forces during the beginning of this project. As a result, some frame parts and the nip adjusters are expected to be slightly oversized. Testing and validation of the calculations will be done in the testing phase to evaluate the calculations and overall performance.

## 6 DESIGN SPECIFICATION

This chapter is used to present the final design, specifications and a cost overview for the material. Parts of the design has been explained in chapter 5. This chapter will describe the total design. A specification of individual parts is described in appendix 4.

### 6.1 TOTAL DESIGN

The machine parts, as described in chapter 5 serve several functions. An overview of the final design is illustrated in Figure 38 and Figure 39.

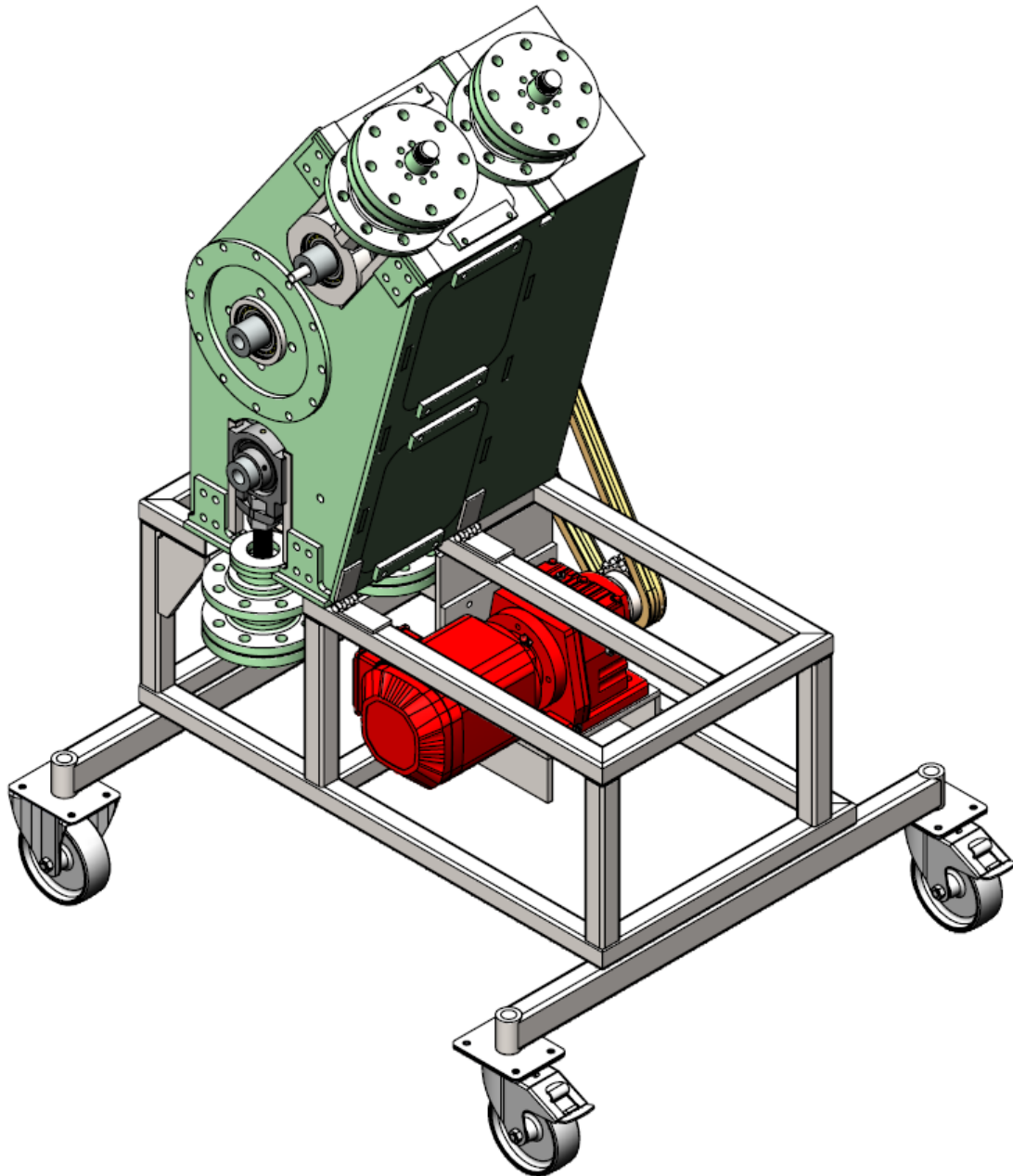


*Figure 38, final design, cooling side*

Figure 38 illustrates the cooling side of the machine. This inlet and outlet of the cooling water is indicated. The rotary joints aren't included in the illustration yet. The inner pipe, for separation of the inlet and outlet flow of cooling water is shown at the upper roller.

The inspection covers are used for cleaning and adjustments in between operations. The roller adjustment mechanisms, including linear bearing housings, spindles and nip adjusters are indicated. The disk spring columns are mounted inside the flanged parts.

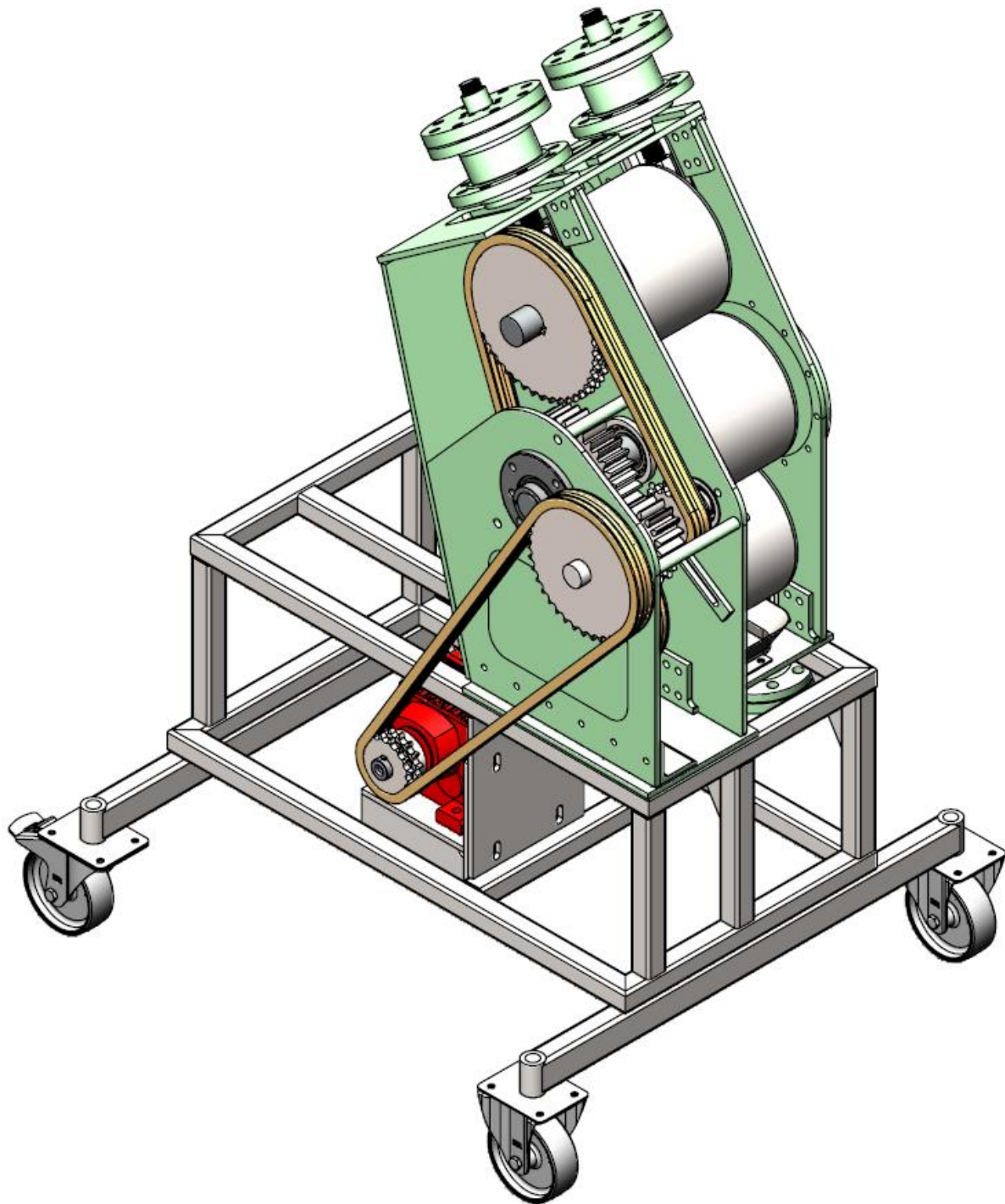


*Figure 39, final design, transmission side*

The motor is mounted in a lower position, in front of the calender, to compensate the higher centre of gravity caused higher mounting position of the calender. Chain tensioners will be installed during assembly. The scrapers are not yet included into the design. Room has been left into the frame for this. The between shaft used for a reduction stage between the rollers and motor/ reductor. Both the upper and bottom roller drive chain and middle roller drive gears are driven by this shaft.

## 6.2 MATERIAL COST OVERVIEW

The development and realisation of the rubber recycling calender was planned to be done during a half year period, starting February 2015. An initial budget of €5000, - was reserved for the development of the rubber recycling calender. This budget was meant to buy parts and materials to fabricate the machine. The feasibility for the realisation of the machine within this budget was unsure.

The realisation is currently in progress. The most expensive components have been ordered at the time of completion of this report. The remaining costs have been estimated according to catalogue prices from various suppliers.

An overview of the total fabrication costs is summarized in Table 20 on the next page. This includes the prices of various parts and outsourcing of fabrication for several components. It doesn't include hours of labour, for in-house fabricated parts.

The total expected amount is estimated around €8548, - for the fabrication of the basic machine. Some additional costs will have to be made for the fabrication of scraping devices and transmission part covers. The airtightness of the machine has to be optimized as well. This can be done by fabricating seals around the inspection cover, and using rubber sheets between the machine frame and extruder output. A total estimation of these additional costs have not yet been made.

The total costs exceeded the initial budget of 5000, -. This was discussed in agreement with the client, and realisation could still continue.

Table 20, Costs overview

<b>Costs made</b>						
<b>Designation</b>	<b>Supplier</b>	<b>type</b>	<b>art.no</b>	<b>Price</b>	<b>quantity</b>	<b>Total price</b>
motor+reductor	Henk Elzing Techniek BV	R57DRE90L4		€ 659,21	1	€ 659,21
Transmission parts	Henk Elzing Techniek BV	various		€ 1.920,28	1	€ 1.920,28
Roller shafts	Klein- Klouwenberg BV	Custom		€ 240,00	3	€ 720,00
Roller sleeve	Metaalketen Hengelo	Custom		€ 242,60	1	€ 242,60
Roller sleeve machining	Hordal BV	Custom		€ 143,39	1	€ 143,39
Roller material steel	Hordal BV	various		€ 512,11	1	€ 512,11
Frame material + cutting	Becker Watersnijtechniek	s355J2 h= 10mm		€ 1.034,55	1	€ 1.034,55
Steel various parts	Ijzerleeuw BV	D= 100/ 180 mm		€ 650,25	1	€ 650,25
Subframe steel	Ijzerleeuw BV	Square tube		€ 54,25	1	€ 54,25
Rotary joints	Brookhuis applied technologies	DP 25R51	1112200-51	€ 298,87	3	€ 896,61
knee pieces rotary joints	Brookhuis applied technologies	PR 2 25G	1112217	€ 45,98	3	€ 137,94
<b>Estimated remaining costs</b>						
frequency converter	ABB			€ 436,60	1	€ 436,60
castor wheels	Conrad		481457	€ 23,00	4	€ 92,00
Trapezium parts	Machinefabriek Harderwijk B.V.	various		€ 105,50	1	€ 105,50
Flanges	Bouwleeuw BV	various		€ 400,00	1	€ 400,00
Disk springs	Alcomex veren BV	various		€ 242,29	1	€ 242,29
Fabrication roller parts	Henk Elzing Techniek BV			€ 300,00	1	€ 300,00
<b>Total price</b>					<b>Incl.</b>	<b>€ 8.547,58</b>

## 7 REALISATION

At the point of completion of this report (01-07-2015), realisation was still in progress. The plan is to complete fabrication of most parts at the beginning of July. Assembly will start the second week of July and completion will be done at the end of July.

Support was gained in fabrication, by a working student in service of the University of Applied Sciences Windesheim. Drawings were supplied to him and he fabricated various parts during the realisation phase. Some complex or larger parts were outsourced to fabricated by various companies.

An overview of various fabricated parts is given in the following pictures.



*Figure 40, Support frame*



Figure 41, Calender frame parts 1

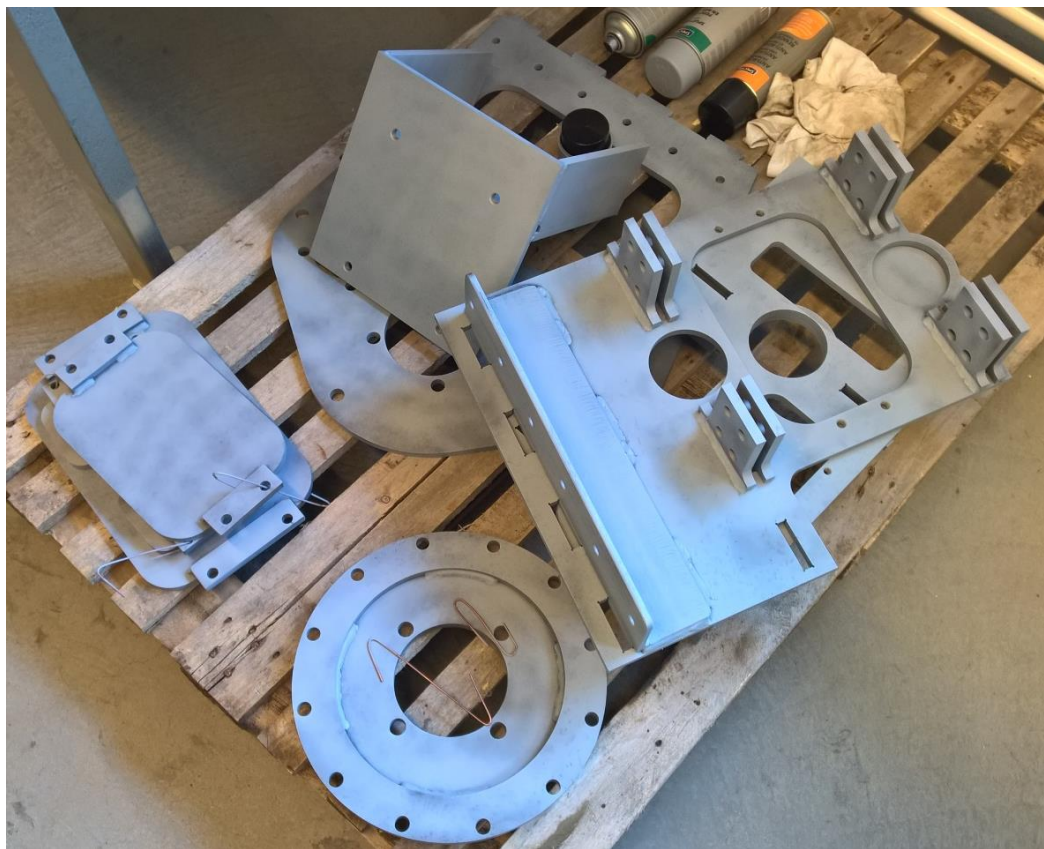


Figure 42, Calender frame parts 2



Figure 43, Roller shaft

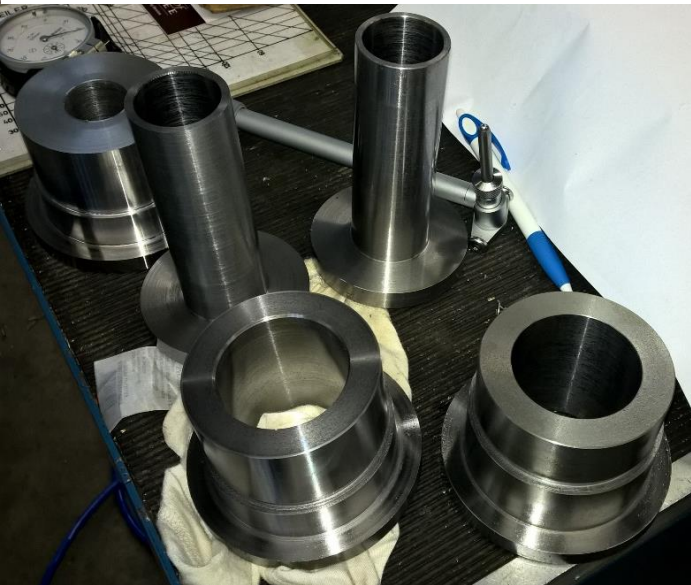


Figure 44, Nip adjuster parts



Figure 45, Transmission parts, gears and sprockets



## 8 CONCLUSIONS AND RECOMMENDATIONS

---

### 8.1 CONCLUSIONS

Laboratory testing and literature research is used to develop a parametric model, used for the development of the cooling calender. It can predict effects on heat exchange when parameters like the rubber flow, nip height and inlet temperature and are changed. The design as described in this report should in theory be able to process a flow of 100 kg/hr of devulcanized rubber, from 250 to 90°C. The necessary parameters are described in this report.

The machine is designed to allow easy adaptation of the roller speed ratios, by changing the amount of teeth of the sprockets. Nip height can be adjusted by turning the nip adjuster nuts. The self-aligning bearings allow the rollers to be adjusted one by one, preventing additional equipment to keep the bearings aligned. Overpressure safeties are included into the nip adjusters to prevent damage of the rollers and construction, when strange object enter the calender. The rollers are designed to allow disassembly. This may be necessary when unexpected damage of the roller surfaces may occur.

The theoretical model has yet to be verified. Testing will be performed using pre-defined parameters, and measurements will be taken of the D-GTR temperatures at various stages of calendering.

The rubber recycling calender is planned to be finished at the beginning of september. Earlier design choices have been made before finalizing certain calculations. Some inaccuracies have been found at the end of this project. The required milling power equation (Eq. 2) has an inaccuracy concerning the mechanical losses. The power should be multiplied by the losses, instead of divided by the losses. As a result, actual milling powers will be lower as initially expected. Parts like drive shafts, gears and chains are slightly oversized for the desired purpose. This has mainly economic consequences and won't affect calendering performance.

The design torque value (Eq. 3) is expected to correspond to a roller diameter of 80 mm. New insights have led to believe that the actual torque value is higher than the initial value, due to the use of larger diameter rollers. This, along with change in power has led to a new value of 390 Nm instead of 520 Nm. This won't cause problems during operations.

Any deviation of the thermal properties of rubber has a large effect on the thermal balance and heat flux. For example, using the same parameters as for the 100 kg/hr case, a drop in diffusivity from  $0.14 \cdot 10^{-7}$  to  $0.12 \cdot 10^{-7}$  m<sup>2</sup>/s, will change the heat flux from 9.35 to 8.18 kW. This means that lower diffusivity values may lower the cooling calender capacity.

The thermal conductivity changes proportional to the thermal conductivity with a constant diffusivity. The available cooling water flow should be able to cool rubber up to 5 kJ/kgK (at 100 kg/hr).

## 8.2 RECOMMENDATIONS

The cooling calender is realised according to the design, as described in this thesis. The machine should, theoretically be able to cool a 100 kg/hr flow of D-GTR from 250 to 90°C. Further testing has to be performed to check the performance, temperatures and rubber calendering properties.

The thermal properties of D-GTR should be measured in a temperature range up to 250°C to make more accurate calculations. Information about the thermal properties of tire rubber is difficult find. The specific heat capacity, thermal diffusivity and conductivity should be determined along the temperature range to exactly calculate the heat flux and amount of heat.

The roller pressures are determined using simulation examples derived from literature during this project. More accurate estimations of the roller pressures can be done by using lubrication equations as in an article by Mitsoulis [16]. These are complex differential equations, considered too complex to use during this project, due to a limited amount of time to implement it into the model.



## 9 BIBLIOGRAPHY

---

- [1] S. Ramarad, M. Khalid, C. Ratnam, A. L. Chuah and W. Rashmi, "Waste tire rubber in polymer blends: A review on the evolution, properties and future," *Progress in Materials Science*, vol. 72, pp. 100--140, 2015.
- [2] S. Saiwari, "Post-consumer tires back into new tires: de-vulcanization and re-utilization of passenger car tires," 2013.
- [3] W. contributors, "Thermal diffusivity," 25 11 2014. [Online]. Available: [https://en.wikipedia.org/wiki/Thermal\\_diffusivity](https://en.wikipedia.org/wiki/Thermal_diffusivity). [Accessed 04 07 2015].
- [4] W. J. Parker, R. J. Jenkins, C. P. Butler and G. L. Abbot, "Flash method of determining thermal diffusivity, heat capacity and thermal conductivity," *Journal of applied physics*, vol. 32, no. 9, pp. 1679 - 1864, 1961.
- [5] G. M. Nasr and M. M. Badawy, "Thermal and Thermoelastic Properties of," vol. 38, pp. 249-255, 1995.
- [6] S. Goyanes, C. Lopez, G. Rubiolo, F. Quasso and A. Marzocca, "Thermal properties in cured natural rubber/styrene butadiene rubber blends," *European Polymer Journal*, vol. 44, no. 5, pp. 1525--1534, 2008.
- [7] J. K. Oleiwi, M. S. Hamza and N. A. Nassir, "A Study of The Effect of Carbon Black Powder on The Physical Properties of SBR/NR Blends Used In Passenger Tire Treads," *Eng. & Tech. Journal*, vol. 29, no. 5, 2011.
- [8] R. Agrawal, N. S. Saxena, G. Mathew, S. Thomas and K. B. Sharma, "Effective Thermal Conductivity of Three-Phase Styrene," *Journal of Applied Polymer Science*, vol. 76, p. 1799--1803, 1999.
- [9] C. Nah, J. H. Park, C. T. Cho, Y.-W. Chang and S. Kaang, "Specific heats of rubber compounds," *Journal of applied polymer science*, vol. 72, no. 12, pp. 1513--1522, 1999.
- [10] toolbox, the engineering, "Thermal properties of water - density, freezing temperature, boiling temperature, latent heat of melting, latent heat of evaporation, critical temperature and more," [Online]. Available: [http://www.engineeringtoolbox.com/water-thermal-properties-d\\_162.html](http://www.engineeringtoolbox.com/water-thermal-properties-d_162.html).
- [11] S. Luther and D. Mewes, "Theoretical study of operating limits for the calendering process," *KGK. Kautschuk, Gummi, Kunststoffe*, vol. 58, no. 4, pp. 149--156, 2005.
- [12] S. Luther, "Berücksichtigung der freien Knetoberfläche beim Berechnen von Stromungsfeldern im Kalanderspalt," *Hamburg, Doktor-Ingenieurin Dissertation*, 2003.
- [13] A. Chorak, E. Ihringer, A. Ben Abdellah, S. Dhimdi, E. H. Essadiqi, M. Bouya and M. Faqir, "Numerical evaluation of heat transfer in corrugated heat exchangers," in *Renewable and Sustainable Energy Conference (IRSEC), 2014 International*, IEEE, 2014, pp. 401 - 406.
- [14] D. Muhs, H. Wittel, M. Becker, D. Jannasch and J. Vossiek, *Roloff/Matek machineonderdelen:*

normering, berekening, vormgeving, Academic Service, 2005.

- [15] Sodemann industriële veren, "<http://www.industriele-veren.nl>," [Online]. Available: <http://www.industriele-veren.nl/online-shop/schotelveren/schotelveren>. [Accessed 2015].
- [16] E. Mitsoulis, "Numerical simulation of calendaring viscoplastic fluids," *Journal of Non-Newtonian Fluid Mechanics*, vol. 154, p. 77–88, 2008.
- [17] S. Chandy, "Studies on vulcanisation kinetics, thermal conductivity and technological properties of aluminium powder-filled natural rubber compounds," 2010.
- [18] R. Grossman, *The Mixing of Rubber*, Springer Science & Business Media, 2012.
- [19] d. W. Dierkes and d. R. Loendersloot, "smart rubber for car tyres," [Online]. Available: <http://www.utwente.nl/time/projects/dm/open/masterassignment-apollovredestein/>.
- [20] K. L. Johnson and J. J. Kauzlarich, "Transfer of material between rolling and sliding surfaces," *International Journal of Mechanical Sciences*, vol. 46, pp. 343 - 357, 2004.
- [21] F. L. Roth, R. L. Driscoll and W. L. Holt, "Frictional properties of rubber," *Rubber Chemistry and Technology*, vol. 16, no. 1, pp. 155--177, 1943.
- [22] P. Sutanto, F. Picchioni and L. Janssen, "Modelling a continuous devulcanization in an extruder," *Chemical engineering science*, vol. 61, no. 21, pp. 7077--7086, 2006.
- [23] Indian Rubber Institute, *Rubber Engineering*, McGraw-Hill Education, 1998.









UNIVERSITY OF TWENTE.

Lectoraat Kunststoftechnologie

Rubber recycling calender  
Hogeschool Windesheim

Peter-Bas  
Schelling